Two-Way Amplify-and-Forward Multiple-Input Multiple-Output Relay Networks with Antenna Selection

Gayan Amarasuriya, *Student Member, IEEE*, Chintha Tellambura, *Fellow, IEEE*, Masoud Ardakani, *Senior Member, IEEE*

***Abstract*—Two new transmit/receive (Tx/Rx) antenna selection strategies are proposed and analyzed for two-way multiple-input multiple-output (MIMO) amplify-and-forward (AF) relay networks. These two strategies select the best transmit and receive antennas at the two sources and the relay based on (i) minimizing the overall outage probability and (ii) maximizing the sum-rate. The performance of these selection strategies is quantified by deriving the overall outage probability, its high SNR approximation and the diversity order providing valuable insights into practical system-designs. Importantly, multiple relay and multiple user two-way relay network set-ups are also treated by proposing and analyzing (i) joint relay and antenna selection strategies, and (ii) joint user, relay and antenna selection strategies, respectively. Interestingly, our outage probability results reveal that the joint relay and antenna selection strategies achieve significant diversity and array gains over those of their single relay counterparts. In fact, the diversity orders of individual relayed-branches accumulate to yield the overall diversity of the multi-relay networks. For example, at 10^{-2} outage probability, the dual-antenna relay provides a 14 dB gain over a single-antenna relay, and having two dual-antenna relays improves the gain by another 5 dB. Moreover, the performance degradation due to practical transmission impairments (i) feedback delays, (ii) spatially-correlated fading and (iii) non-identically distributed fading is quantified. Impact of channel prediction to circumvent outdated channel state information for antenna selection due to feedback delay is also studied. All the derivations are validated through Monte-Carlo simulations.**

***Index Terms*—Two-way relay networks, Amplify-and-forward, MIMO, Antenna selection**

I. Introduction

TWO-WAY relaying is a promising spectral efficient transmission protocol for wireless networks with half-duplex terminals [1]–[5]. Specifically, two-way relay networks (TWRNs) avoid the pre-log factor of one-half in capacity expressions, and thus, are twice as spectrally efficient as the conventional one-way relay networks [1], [2]. The performance of TWRNs can be further improved by integrating multiple-input multiple-output (MIMO) transmission technology [6]–[9]. However, the main drawback of any MIMO system is the increased system complexity due to the additional cost for enabling multiple transmit and receive radio frequency (RF) chains[1] [10]. Antenna selection for single-hop MIMO systems has been widely studied to circumvent these drawbacks [10]. In particular, antenna selection reduces the complexity and the power requirements of the MIMO transmitter much more than most other transmit diversity schemes such as beamforming [11]. In this paper, two new transmit/receive (Tx/Rx) strategies are proposed for MIMO amplify-and-forward (AF) TWRNs[2].

Prior related research: In the wide body of relay literature, there appear only two studies, [12] and [13], dealing with the issue of antenna selection for TWRNs. In [12], the upper bounds for the average symbol error probability of network-coded decode-and-forward (DF) TWRNs having two single-antenna sources and a dual-antenna relay are studied. In [12], during the first time-slot, two independent symbols are transmitted simultaneously by both sources to the relay. At the relay, these two symbols are decoded separately, and in the second time-slot, the relay transmits a physical layer network-coded symbol (the XOR of the two symbols) to the two sources by using Alamouti coding or antenna selection. Reference [13] extends the results of [12] by using either max-min antenna selection or maximal ratio transmission in the second time-slot. In particular, the transmission strategy in [13] achieves a diversity gain in the order of the number of antennas at the relay.

In addition to the above studies, [6]–[8] investigate the designing of optimal transmit precoders and receiver filters for MIMO TWRNs with the availability of perfect channel state information (CSI). Moreover, [9] studies the effects of channel estimation errors on the receivers of MIMO AF TWRNs.

For the sake of completeness, we also mention the prior related research on single-antenna TWRNs. References [4], [14] provide rigorous analyses of the practical physical layer network coding for TWRNs, and thereby, quantify the outage probability, sum-rate and corresponding high SNR approximations. In [5], [15], [16], various relay selection schemes for multi-relay TWRNs are studied.

Motivation and our contribution: References [12], [13] investigate antenna selection only for DF TWRNs, where individual symbols from the two sources are first decoded separately and then a network-coded symbol is broadcast back to these sources. In particular, the system models in both [12][3]

Manuscript received 1 August 2011; revised 1 May 2012. This work was supported by the Alberta Innovates Technology Futures Graduate Student Scholarship Program. This work in part has been presented in IEEE Global Commun. Conf. (GLOBCOM), Houston, Texas, USA, Dec. 2011.

The authors are with the Department of Electrical and Computer Engineering, University of Alberta, Edmonton, AB, Canada T6G 2V4 (e-mail: {amarasur, chintha, ardakani}@ece.ualberta.ca.).

Digital Object Identifier 10.1109/JSAC.2012.120919.

[1]Passive antenna elements and additional digital signal processing are becoming increasingly cheaper; however, RF elements are still expensive and do not follow Moore's law [10].

[2]Amplify-and-forward two-way relaying is also known as analog network coding [2], [6].

[3]The system model in [12] is restricted to a dual-antenna relay terminal.

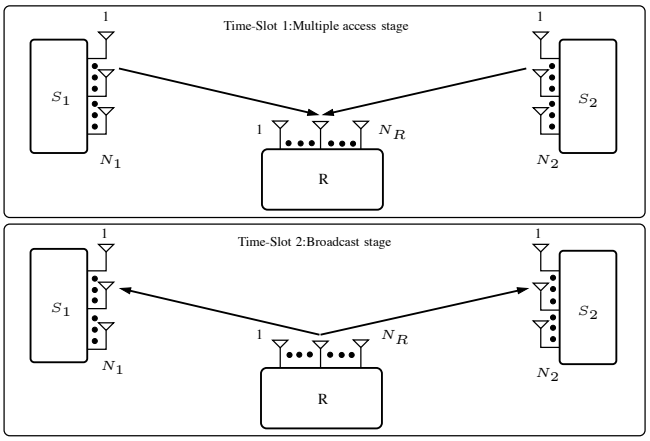

Fig. 1. A MIMO AF TWRN with Tx/Rx antenna selection

and [13] employ multiple antennas at the relay only, and each source is equipped with a single antenna. Furthermore, in [12], [13], the transmit antenna selection is considered in the second time-slot (broadcast phase) only. The precoder/decoder designs proposed in [6]–[9] require employing multiple Tx/Rx RF chains at each terminal, and hence, increase both complexity and cost, which clearly loosens one of the main trade-offs of deploying relay networks; i.e., the cost versus performance.

Therefore, to the best of our knowledge, both Tx/Rx antenna selection for single-relay MIMO AF TWRNs, and joint relay and antenna selection for multi-relay MIMO AF TWRNs have not yet been studied. This paper fills this gap by proposing two new Tx/Rx antenna selection strategies for MIMO AF TWRNs, where each terminal is equipped with multiple-antennas. Specifically, the first selection strategy (SS-1) selects the best Tx/Rx antennas at the two sources and relay based on maximizing the end-to-end signal-to-noise ratio (e2e SNR) of the worst source, and hence, minimizing the overall outage probability. In contrast, the key design criterion of the second selection strategy (SS-2) is the maximization of the sum-rate. Notably, both these strategies achieve the full diversity order. Moreover, two useful generalizations (i) a multi-relay system set-up, and (ii) a multi-relay and multi-user system set-up are also treated by proposing and analyzing the corresponding joint relay and Tx/Rx antenna selection strategies. The other main contributions of our work can be listed as follows:

1) The performance of the proposed transmission strategies over frequency-flat Rayleigh fading is studied by deriving the overall outage probability and its high SNR approximation.
2) The diversity orders of the proposed transmission strategies are derived to show the optimality, and to obtain valuable insights into practical system-design.
3) In particular, the performance of the two selection strategies is compared in terms of the outage probability of the worst source and the average sum-rate.
4) The performance degradations due to three important practical transmission impairments (i) feedback delays, (ii) spatially-correlated fading, and (iii) non-identically distributed fading are quantified.
5) Specifically, The detrimental effect of feedback delays on the performance of antenna selection is also quantified. To this end, the exact outage probability, its high SNR approximation and the diversity order of SS-1 are derived for Tx/Rx antennas selection based on outdated channel state information (CSI) due to feedback delays.
6) The impact of channel prediction to circumvent the adverse effects of outdated CSI is also studied by presenting and analyzing a linear finite impulse response (FIR) channel prediction strategy for MIMO TWRNs.
7) The asymptotic performance degradation due to spatially-correlated Rayleigh fading among multiple antenna elements is quantified to obtain valuable insights into practical system-design.
8) Furthermore, the effect of non-identically distributed fading on the system performance is investigated by deriving the exact overall outage probability and its asymptotic high SNR approximation.
9) Insightful numerical results are provided to show the performance gains of the proposed strategies, and our analysis is validated through Monte-Carlo simulations.

The rest of this paper is organized as follows: Sections II and III present the system model and problem formulation of two Tx/Rx antenna selection strategies, respectively. Section IV presents the exact and asymptotic outage probability analysis. Sections V and VI provide the problem formulation and its performance analysis of multi-relay and multi-relay/multi-user generalizations, respectively. In Section VII, the effect of practical transmission impairments on the system performance is studied. Section VIII contains the numerical and simulation results. Section IX presents our conclusions.

II. System model

We consider a MIMO AF TWRN (see Fig. 1) consisting of two source nodes (S_1 and S_2), and one relay node (R). Specifically, S_1, S_2 and R are equipped with N_1, N_2 and N_R antennas, respectively. All nodes are assumed to be half-duplex, and all channel amplitudes are assumed to be independently distributed frequency-flat Rayleigh fading. The feedbacks for antenna selection are assumed to be perfect unless otherwise stated. The channel matrix from $S_i|_{i=1}^2$ to R is denoted by $H_{S_iR}|_{i=1}^2$. In particular, all the channel coefficients are assumed to be fixed over two consecutive time-slots unless otherwise stated [1]. Thus, the channels matrix from R to $S_i|_{i=1}^2$ can be denoted as $(H_{S_iR})^T|_{i=1}^2$. Further, the (k,l)-th element[4] of H_{S_iR} is denoted by $h_{S_iR}^{k,l}$ and modeled as $h_{S_iR}^{k,l} \sim \mathcal{CN}(0,\zeta_i)$. Here, $\zeta_i|_{i=1}^2$ accounts for the path-loss effect and is modeled as $\zeta_i \propto (d_{S_iR})^{-\varpi_i}$, where $d_{S_iR}|_{i=1}^2$ is the distance between S_i and R, and $\varpi|_{i=1}^2$ is the path-loss exponent of $S_i \rightarrow R$ channel. The additive noise at all the receivers is modeled as complex zero mean white Gaussian noise. The direct channel between S_1 and S_2 is assumed to be unavailable due to heavy path-loss and shadowing [1], [4].

In this protocol, S_1 and S_2 exchange their information-bearing symbols[5], $\mathcal{X}_1$ and $\mathcal{X}_2$, respectively, in two time-slots. In the first time-slot, both S_1 and S_2 transmit $\mathcal{X}_1$ and $\mathcal{X}_2$ simultaneously by selecting the jth and lth transmit antennas,

[4]Here, $h_{S_iR}^{k,l}$ is the channel coefficient from the lth transmit antenna of S_i to the kth receive antenna of R.

[5]The information-bearing symbols have unit symbol energies; i.e., $\mathcal{E}\{|\mathcal{X}_1|^2\} = 1$ and $\mathcal{E}\{|\mathcal{X}_2|^2\} = 1$.

respectively, to R over a multiple access channel. Then R receives the superimposed-signal[6] by selecting the mth receive antenna as follows:

$$Y_R = \sqrt{\mathcal{P}_{S_1}} h_{S_1R}^{m,j} \mathcal{X}_1 + \sqrt{\mathcal{P}_{S_2}} h_{S_2R}^{m,l} \mathcal{X}_2 + n_R, \quad (1)$$

where $\mathcal{P}_{S_i}|_{i=1}^2$ is the transmit power of S_i, and n_R is the additive white Gaussian noise (AWGN) at R having mean zero and variance σ_R^2. In the second time slot, R amplifies Y_R with a gain $G = \sqrt{\mathcal{P}_R/(\mathcal{P}_{S_1}\left|h_{S_1R}^{m,j}\right|^2 + \mathcal{P}_{S_2}\left|h_{S_2R}^{m,l}\right|^2 + \sigma_R^2)}$ and then broadcasts it again by using the mth transmit antenna to $S_i|_{i=1}^2$ over the broadcast channel. Here, $\mathcal{P}_R$ is the transmit power at R. Then, S_1 and S_2 receive the signal by again using the jth and lth receive antennas[7], respectively, as follows:

$$Y_{S_1} = G h_{S_1R}^{m,j} Y_R + n_1 \quad \text{and} \quad Y_{S_2} = G h_{S_2R}^{m,l} Y_R + n_2, \quad (2)$$

where $n_i|_{i=1}^2 \sim \mathcal{CN}\left(0, \sigma_i^2\right)$ is the AWGN at S_i. By substituting (1) into (2) and removing the self-interference[8] [1], the e2e SNR at $S_i|_{i=1}^2$ can be derived as

$$\gamma_{S_1}^{(j,l,m)} = \frac{\left(\frac{\mathcal{P}_R|h_{S_1R}^{m,j}|^2}{\sigma_1^2}\right)\left(\frac{\mathcal{P}_{S_2}|h_{S_2R}^{m,l}|^2}{\sigma_R^2}\right)}{\left(\frac{\mathcal{P}_R}{\sigma_1^2} + \frac{\mathcal{P}_{S_1}}{\sigma_R^2}\right)|h_{S_1R}^{m,j}|^2 + \frac{\mathcal{P}_{S_2}|h_{S_2R}^{m,l}|^2}{\sigma_R^2} + 1} \quad \text{and}$$

$$\gamma_{S_2}^{(j,l,m)} = \frac{\left(\frac{\mathcal{P}_{S_1}|h_{S_1R}^{m,j}|^2}{\sigma_2^2}\right)\left(\frac{\mathcal{P}_R|h_{S_2R}^{m,l}|^2}{\sigma_R^2}\right)}{\frac{\mathcal{P}_{S_1}|h_{S_1R}^{m,j}|^2}{\sigma_R^2} + \left(\frac{\mathcal{P}_R}{\sigma_2^2} + \frac{\mathcal{P}_{S_2}}{\sigma_R^2}\right)|h_{S_2R}^{m,l}|^2 + 1}. \quad (3)$$

In the next section, the optimal selection of antenna indices (j, l, and m) is described in detail.

III. Problem Formulation

In this section, two novel antenna selection strategies are proposed for MIMO AF TWRNs. The two key design criteria are the joint selection of the best single transmit and receive antennas at S_1, S_2 and R based on (i) minimizing the overall outage probability and (ii) maximizing the sum-rate.

A. Selection strategy-1 (SS-1): Minimization of the overall outage probability

The overall performance of multi-source systems is governed by the performance of the weakest source [17]. Thus, our system is in outage if either S_1 or S_2 is in outage. This observation motivates our antenna selection criterion: the joint maximization of the e2e SNR of the weakest source. To this end, the antenna indices at S_1, S_2 and R are selected to maximize the e2e SNR of the worst source, and there by, to minimize the overall system outage probability[9] as follows:

$$\{J, L, M\} = \underset{\substack{1\le j\le N_1, 1\le l\le N_2 \\ 1\le m\le N_R}}{\operatorname{argmax}} \left[\min\left(\gamma_{S_1}^{(j,l,m)}, \gamma_{S_2}^{(j,l,m)}\right)\right], \quad (4)$$

where J, L, and M are the best antenna indices at S_1, S_2 and R, respectively[10], which minimize the overall outage probability of the two-way MIMO AF relay network.

B. Selection strategy-2 (SS-2):Maximization of the sum-rate

Alternatively, the overall sum-rate of multi-source systems is an important performance metrics. Thus, we consider maximizing the sum-rate of S_1 and S_2 by jointly selecting the best Tx/Rx antennas at S_1, S_2, and R. The instantaneous sum-rate of S_1 and S_2 is given by

$$\mathcal{R}^{(j,l,m)} = \frac{1}{2}\log\left(1+\gamma_{S_1}^{(j,l,m)}\right) + \frac{1}{2}\log\left(1+\gamma_{S_2}^{(j,l,m)}\right) = \frac{1}{2}\log\left(\left(1+\gamma_{S_1}^{(j,l,m)}\right)\left(1+\gamma_{S_2}^{(j,l,m)}\right)\right). \quad (5)$$

By using (5), the antenna selection criterion can be given by

$$\{J, L, M\} = \underset{\substack{1\le j\le N_1, 1\le l\le N_2 \\ 1\le m\le N_R}}{\operatorname{argmax}} \left[\left(1+\gamma_{S_1}^{(j,l,m)}\right)\left(1+\gamma_{S_2}^{(j,l,m)}\right)\right], \quad (6)$$

where J, L, and M are best antenna indices at S_1, S_2 and R, respectively, which maximize the sum-rate of the two-way MIMO AF relay network.

IV. Performance Analysis

In this section, the performance of the proposed antenna selection strategies is studied. In particular, the high SNR approximation of the outage probability is derived to obtain valuable insights about the system-design parameters such as the diversity order and the array gain.

A. Overall outage probability

The overall outage probability of the two selection strategies given in (4) and (6) is studied in the subsequent subsections.

1) Overall outage probability of SS-1: The overall outage probability (P_{out}) of SS-1 (4), is defined as the probability that the instantaneous e2e SNR of the weakest source falls below a preset threshold γ_{th}[11]. Thus, P_{out} is given by

$$P_{out} = \Pr\left[Z = \max_{\substack{1\le j\le N_1, 1\le l\le N_2 \\ 1\le m\le N_R}} \left\{\min\left(\gamma_{S_1}^{(j,l,m)}, \gamma_{S_2}^{(j,l,m)}\right)\right\} \le \gamma_{th}\right]. \quad (7)$$

In order to evaluate P_{out} in closed-form, the cumulative distribution function (CDF) of the random variable Z should

[6]This superimposed-signal is also known as the analog network code in the two-way relay networks [2], [6].

[7]In the second phase, one would alternatively select the antenna tuple (j', l', m') at S_1, S_2, and R, respectively, which are not necessarily same as (j, l, m). However, the overall achievable diversity order would be the same for both the cases.

[8]It is assumed that S_i knows its own information-bearing symbol $\mathcal{X}_i$ and all the channel coefficients.

[9]Alternatively, this strategy can be seen as the maximization of the instantaneous mutual information (IMI) of the worst source. Equivalently, $\{J, L, M\} = \underset{\substack{1\le j\le N_1, 1\le l\le N_2 \\ 1\le m\le N_R}}{\operatorname{argmax}} \left[\min\left(\mathcal{I}_{S_1}^{(j,l,m)}, \mathcal{I}_{S_2}^{(j,l,m)}\right)\right]$, where $\mathcal{I}_{S_1}^{(j,l,m)} = \frac{1}{2}\log\left(1+\gamma_{S_1}^{(j,l,m)}\right)$ and $\mathcal{I}_{S_2}^{(j,l,m)} = \frac{1}{2}\log\left(1+\gamma_{S_2}^{(j,l,m)}\right)$ are the IMI at S_1 and S_2, respectively.

[10]Since the channel matrices, H_{S_1R} and H_{S_2R}, remain static over the two time-slots, S_1, S_2 and R can use the Jth, Lth and Mth antennas, respectively, for both transmission and reception.

[11]Similarly, the information outage probability can be defined as follows: $P_{out} = \Pr\left[\max_{1\le j\le N_1, 1\le l\le N_2, 1\le m\le N_R} \left\{\min\left(\mathcal{I}_{S_1}^{(j,l,m)}, \mathcal{I}_{S_2}^{(j,l,m)}\right)\right\} \le \frac{R_{th}}{2}\right]$, where R_{th} is the target rate of the whole system, and $\mathcal{I}_{S_i}^{(j,l,m)}\Big|_{i=1}^2 = \frac{1}{2}\log\left(1+\gamma_{S_i}^{(j,l,m)}\right)$ is the instantaneous mutual information at S_i. Here, the target rate of each source is set to $\frac{R_{th}}{2}$. Thus, the outage probability is given by $P_{out} = \Pr\left[\frac{1}{2}\log\left(1+Z\right) \le \frac{R_{th}}{2}\right] = \Pr\left[Z \le 2^{R_{th}} - 1\right]$, where $Z = \max_{1\le j\le N_1, 1\le l\le N_2, 1\le m\le N_R} \left\{\min\left(\gamma_{S_1}^{(j,l,m)}, \gamma_{S_2}^{(j,l,m)}\right)\right\}$.

$$F(z,a,b,c,d,u,v)=\sum_{p=0}^{N_1-1}\sum_{q=0}^{N_2-1}\frac{N_1N_2\binom{N_1-1}{p}\binom{N_2-1}{q}(-1)^{p+q}}{b\zeta_1\zeta_2}\left[\frac{1-\mathrm{e}^{-a\beta z}}{a}-\frac{1-\mathrm{e}^{-(a+b)\beta z}}{a+c}\right]+\sum_{p=0}^{u}\sum_{q=0}^{v}d\binom{u}{p}\binom{v}{q}(-1)^{p+q}\left[\frac{\mathrm{e}^{-(a+c)\beta z}(1-\mathrm{e}^{-(a+c)\phi(z)})}{a+c}-\frac{\mathrm{e}^{-(a\phi(z)+(a\beta+c\alpha)z)}}{a}\mathcal{J}(z)\right]. \quad (9)$$

be first derived, and then evaluate this CDF at γ_{th}. Thus, the CDF of Z is given by (see Appendix A for the proof)

$$F_Z(z)=\left[F\left(z,\frac{p+1}{\zeta_1},\frac{q+1}{\zeta_2},\frac{q}{\zeta_2},\frac{N_1}{\zeta_1},N_1-1,N_2\right)+F\left(z,\frac{q+1}{\zeta_2},\frac{p+1}{\zeta_1},\frac{p}{\zeta_1},\frac{N_2}{\zeta_2},N_1,N_2-1\right)\right]^{N_R}, \quad (8)$$

where $F(z,a,b,c,d,u,v)$ is given by (9). In (9), $\alpha=\frac{\bar{\gamma}_S\bar{\gamma}_R}{\bar{\gamma}_R+\bar{\gamma}_T}$, $\beta=\frac{1}{\bar{\gamma}_R}$, $\phi(z)=\frac{1}{\bar{\gamma}_S\bar{\gamma}_R}\sqrt{(\bar{\gamma}_S^2+\bar{\gamma}_S\bar{\gamma}_R+\bar{\gamma}_R^2/4)z^2+\bar{\gamma}_S\bar{\gamma}_Rz}+\frac{z}{2\bar{\gamma}_S}$. Further, $\mathcal{J}(z)$ in (9) can be given in two forms as follows: (I) By using Gauss-Laguerre quadrature (GLQ) [18, Eq. (25.4.45)], $\mathcal{J}(z)$ can be evaluated as $\mathcal{J}(z)=\sum_{t=1}^{T_g}w_t\mathrm{e}^{-\frac{acz(\alpha\beta z+\eta)}{x_t+a\phi(z)}}+\mathcal{R}_{T_g}$, where $\eta=\frac{1}{\bar{\gamma}_S\bar{\gamma}_S}$. Here, $x_t|_{t=1}^{T_g}$ and $w_t|_{t=1}^{T_g}$ are the abscissas and weights of the GLQ, respectively, and they can be efficiently computed by using the classical algorithm in [19] (see Appendix A for more details). Moreover, T_g is the number of terms used for the GLQ, and $\mathcal{R}_{T_g}$ is the remainder term, which diminishes as T_g approaches as small as 10 [19]. (II) Alternatively, by using Taylor series expansion, $\mathcal{J}(z)$ can be derived as $\mathcal{J}(z)=\sum_{i=0}^{\infty}\frac{(-1)^i}{i!}(acz(\alpha\beta z+\eta))^i\mathrm{e}^{a\phi(z)}\Gamma(1-i,a\phi(z))$. The convergence of the infinite series in $\mathcal{J}(x)$ is discussed in Appendix A.

Next, the overall outage probability can be derived readily by evaluating the CDF of Z in (8) at the threshold γ_{th} as follows: $P_{out}=F_Z(\gamma_{th})$.

2) Overall outage probability of SS-2: The outage probability of the SS-2 (6) can be defined as the probability that the instantaneous sum-rate falls below a target rate R_{th}, and given by

$$P_{out}=\Pr\left[\underset{\substack{1\le j\le N_1,1\le l\le N_2\\1\le m\le N_R}}{\operatorname{argmax}}\mathcal{R}^{(j,l,m)}\le R_{th}\right]=\Pr\left[W\le 2^{2R_{th}}-1\right], \quad (10a)$$

where W is given by

$$W=\max_{\substack{1\le j\le N_1,1\le l\le N_2\\1\le m\le N_R}}\left\{\gamma_{S_1}^{(j,l,m)}+\gamma_{S_2}^{(j,l,m)}+\gamma_{S_1}^{(j,l,m)}\gamma_{S_2}^{(j,l,m)}\right\}. \quad (10b)$$

The CDF of an asymptotically-exact upper bound of W can be derived as (see Appendix B for the proof)

$$F_{W^{ub}}(w)=\sum_{a=0}^{N_R}\sum_{b=0}^{a}\sum_{c=0}^{a}\sum_{d=0}^{bN_1}\sum_{e=0}^{cN_2}(-1)^{a+b+c+d+e}\times\binom{N_R}{a}\binom{a}{b}\binom{a}{c}\binom{bN_1}{d}\binom{cN_2}{e}\mathrm{e}^{-\xi\sqrt{\frac{w}{\nu}}}, \quad (11)$$

where $\nu=\frac{\bar{\gamma}_S\bar{\gamma}_R^2}{\bar{\gamma}_S+\bar{\gamma}_R}$ and $\xi=\frac{d}{\zeta_1}+\frac{e}{\zeta_2}$. A lower bound for the overall outage probability of SS-2 can now be obtained by evaluating (11) at $2^{2R_{th}}-1$.

B. High SNR approximation of the overall outage probability

To obtain direct insights, the high SNR approximations of the overall outage probability for SS-1 and SS-2 are derived, and thereby, the corresponding diversity orders are quantified.

1) High SNR approximation of the overall outage probability for SS-1: The high SNR approximation of the overall outage probability is given by (see Appendix C for the proof)

$$P_{out}^{\infty}=\Omega\left(\frac{\gamma_{th}}{\bar{\gamma}}\right)^{G_d}+o\left(\bar{\gamma}^{-(G_d+1)}\right), \quad (12a)$$

where G_d is the diversity order and given by

$$G_d=N_R\min(N_1,N_2). \quad (12b)$$

Furthermore, the system-dependent parameter Ω is given by

$$\Omega=\begin{cases}\left(\frac{C_S+C_R}{\zeta_1C_SC_R}\right)^{N_1N_R}, & N_1<N_2\\ \left(\frac{C_S+C_R}{\zeta_2C_SC_R}\right)^{N_2N_R}, & N_1>N_2\\ \left(\frac{1}{\zeta_1^N}+\frac{1}{\zeta_2^N}\right)^{N_R}\left(\frac{C_S+C_R}{C_SC_R}\right)^{NN_R}, & N_1=N_2=N,\end{cases} \quad (12c)$$

where C_S and C_R are the ratios of the source and relay average transmit SNR to the reference average transmit SNR ($\bar{\gamma}$), respectively; i.e., $C_S=\frac{\bar{\gamma}_S}{\bar{\gamma}}$ and $C_R=\frac{\bar{\gamma}_R}{\bar{\gamma}}$.

2) High SNR approximation of the overall outage probability for SS-2: The high SNR approximation of the outage probability can be derived as (see Appendix D for the proof)

$$P_{out}^{\infty}=\Delta\left(\frac{\sqrt{2^{2R_{th}}-1}}{\bar{\gamma}}\right)^{G_d}+o\left(\bar{\gamma}^{-(G_d+1)}\right), \quad (13a)$$

where the diversity order of SS-2 is the same as that of SS-1 given in (12b). Moreover, Δ is given by

$$\Delta=\begin{cases}\left(\frac{2[C_S+C_R]}{\zeta_1^2C_SC_R^2}\right)^{\frac{N_1N_R}{2}}, & N_1<N_2\\ \left(\frac{2[C_S+C_R]}{\zeta_2^2C_SC_R^2}\right)^{\frac{N_2N_R}{2}}, & N_1>N_2\\ \left(\frac{1}{\zeta_1^N}+\frac{1}{\zeta_2^N}\right)^{N_R}\left(\frac{2[C_S+C_R]}{C_SC_R^2}\right)^{\frac{NN_R}{2}}, & N_1=N_2=N,\end{cases} \quad (13b)$$

where C_S and C_R are defined in (12c).

V. Joint relay and antenna selection

In this section, our proposed antenna selection strategies are extended to two-way MIMO AF multi-relay networks. Here, we consider a MIMO AF TWRN having two source nodes, S_1 and S_2, and K number of potential relays ($R_k|_{k=1}^K$), each equipped with N_1, N_2 and $N_{R_k}|_{k=1}^K$ antennas, respectively. The key design criterion is the joint selection of the best relay (R_{K^*}), and the best antenna indices, J, K, and M_{K^*} of S_1, S_2 and R_{K^*}, respectively, (i) to minimize the overall outage probability, and (ii) to maximize the sum-rate.

A. Joint relay and antenna selection for SS-1

The joint relay and antenna selection criterion for maximizing the e2e SNR of the worst source, and thereby, for minimizing the overall outage probability is given by

$$\{J, L, K^*, M_{K^*}\} = \underset{\substack{1\le j\le N_1, 1\le l\le N_2 \\ 1\le k\le K, 1\le m_k\le N_{R_k}}}{\operatorname{argmax}} \left[\min\left(\gamma_{S_1}^{(j,l,m_k)}, \gamma_{S_2}^{(j,l,m_k)}\right)\right] \quad (14)$$

Next, the corresponding overall outage probability can be readily derived by using (8) as follows:

$$P_{out} = \prod_{k=1}^{K}\left\{\left[F\left(\gamma_{th}, \frac{p+1}{\zeta_{1,k}}, \frac{q+1}{\zeta_{2,k}}, \frac{q}{\zeta_{2,k}}, \frac{N_1}{\zeta_{1,k}}, N_1-1, N_2\right) + F\left(\gamma_{th}, \frac{q+1}{\zeta_{2,k}}, \frac{p+1}{\zeta_{1,k}}, \frac{p}{\zeta_{1,k}}, \frac{N_2}{\zeta_{2,k}}, N_1, N_2-1\right)\right]^{N_{R_k}}\right\}, \quad (15)$$

where $F(\cdot,\cdot,\cdot,\cdot,\cdot)$ is given by (9) after replacing ζ_1, ζ_2, N_R, α, β, and $\phi(z)$ with $\zeta_{1,k}$, $\zeta_{2,k}$, N_{R_k}, $\alpha_k = \frac{\bar{\gamma}_S+\bar{\gamma}_{R_k}}{\bar{\gamma}_S\bar{\gamma}_{R_k}}$, $\beta_k = \frac{1}{\bar{\gamma}_{R_k}}$ and $\phi_k(z) = \frac{1}{\bar{\gamma}_S\bar{\gamma}_{R_k}}\sqrt{(\bar{\gamma}_S^2 + \bar{\gamma}_S\bar{\gamma}_{R_k} + \bar{\gamma}_{R_k}^2/4)z^2 + \bar{\gamma}_S\bar{\gamma}_{R_k}z} + \frac{z}{2\bar{\gamma}_S}$, respectively.

The asymptotic outage probability at high SNRs for the joint antenna and relay selection can be derived by using (12a) as follows:

$$P_{out}^{\infty} = \left(\prod_{k=1}^{K}\Omega_k\right)\left(\frac{\gamma_{th}}{\bar{\gamma}}\right)^{\sum_{k=1}^{K}G_{d_k}} + o\left(\bar{\gamma}^{-(\sum_{k=1}^{K}G_{d_k}+1)}\right), \quad (16a)$$

where the diversity order G_d is given by

$$G_d = \sum_{k=1}^{K}G_{d_k} = \min(N_1, N_2)\sum_{k=1}^{K}N_{R_k}. \quad (16b)$$

In (16a), Ω_k is obtained again by replacing ζ_1, ζ_2 and C_R of (12c) with $\zeta_{1,k}$, $\zeta_{2,k}$ and $C_{R_k} = \frac{\bar{\gamma}_{R_k}}{\bar{\gamma}}$, respectively.

B. Joint relay and antenna selection for SS-2

The joint relay and antenna selection criterion for maximizing the sum-rate is given by

$$\{J, L, K^*, M_{K^*}\} = \underset{\substack{1\le j\le N_1, 1\le l\le N_2 \\ 1\le k\le K, 1\le m_k\le N_{R_k}}}{\operatorname{argmax}} \left[\gamma_{S_1}^{(j,l,m_k)} + \gamma_{S_2}^{(j,l,m_k)} + \gamma_{S_1}^{(j,l,m_k)}\gamma_{S_2}^{(j,l,m_k)}\right]. \quad (17)$$

The resulting outage probability upper bound can be obtained readily by using (11) as follows:

$$P_{out}^{ub} = \left[\sum_{a=0}^{N_{R_k}}\sum_{b=0}^{a}\sum_{c=0}^{a}\sum_{d=0}^{bN_1}\sum_{e=0}^{cN_2}(-1)^{a+b+c+d+e} \times \binom{N_R}{a}\binom{a}{b}\binom{a}{c}\binom{bN_1}{d}\binom{cN_2}{e}\mathrm{e}^{-\xi_k\sqrt{\frac{w}{\nu_k}}}\right]^{N_{R_k}}, \quad (18)$$

where $\nu_k = \frac{\bar{\gamma}_S\bar{\gamma}_{R_k}^2}{\bar{\gamma}_S+\bar{\gamma}_{R_k}}$ and $\xi_k = \frac{d}{\zeta_{1,k}} + \frac{e}{\zeta_{k,2}}$.

The asymptotic outage probability of (18) at high SNRs can be derived by using (13a) as

$$P_{out}^{\infty} = \left(\prod_{k=1}^{K}\Delta_k\right)\left(\frac{\sqrt{2^{2R_{th}}}}{\bar{\gamma}}\right)^{\sum_{k=1}^{K}G_{d_k}} + o\left(\bar{\gamma}^{-(\sum_{k=1}^{K}G_{d_k}+1)}\right), \quad (19)$$

where the diversity order is the same as that of joint relay and antenna selection for SS-1 and given by (16b). Further, Δ_k in (19) can be obtained by replacing ζ_1, ζ_2 and C_R of (13b) with $\zeta_{1,k}$, $\zeta_{2,k}$ and C_{R_k}, respectively.

VI. Multi-user MIMO AF TWRNs with antenna selection

In this section, our selection strategies are extended to treat multiuser multi-relay TWRNs. To this end, we consider a MIMO AF TWRN with two groups of users ($\mathcal{U}$ and $\mathcal{V}$) communicating opportunistically over multiple relays $\left(R_k|_{k=1}^{K}\right)$. Specifically, the user groups $\mathcal{U}$ and $\mathcal{V}$ consist of U and V users and are denoted as $S_{1,u}|_{u=1}^{U}$ and $S_{2,v}|_{v=1}^{V}$, respectively. In this context, two joint user, relay and antenna selection strategies based on the overall outage probability minimization and sum-rate maximization are developed.

A. Joint user, relay and antenna selection for SS-1

The joint user, relay and antenna selection criterion for minimizing the overall outage probability is given by

$$\{J, L, K^*, M_{K^*}, U^*, V^*\} = \underset{\substack{1\le j\le N_1, 1\le l\le N_2, 1\le k\le K \\ 1\le m_k\le N_{R_k}, 1\le u\le U, 1\le v\le V}}{\operatorname{argmax}} \left[\min\left(\gamma_{S_1}^{(j,l,m_k,u,v)}, \gamma_{S_2}^{(j,l,m_k,u,v)}\right)\right]. \quad (20)$$

B. Joint user, relay and antenna selection for SS-2

The joint user, relay and antenna selection criterion for maximizing the sum-rate is given by

$$\{J, L, K^*, M_{K^*}, U^*, V^*\} = \underset{\substack{1\le j\le N_1, 1\le l\le N_2, 1\le k\le K \\ 1\le m_k\le N_{R_k}, 1\le u\le U, 1\le v\le V}}{\operatorname{argmax}} \left[\gamma_{S_1}^{(j,l,m_k,u,v)} + \gamma_{S_2}^{(j,l,m_k,u,v)} + \gamma_{S_1}^{(j,l,m_k,u,v)}\gamma_{S_2}^{(j,l,m_k,u,v)}\right]. \quad (21)$$

Remark IV.1: The overall outage probability for both SS-1 and SS-2 strategies can readily be derived by replacing N_1 and N_2 by UN_1 and VN_2 in (15) and (18), respectively[12]. Moreover, the corresponding high SNR approximations can be similarly obtained first by performing the aforementioned substitution and then replacing G_d by $G_d = \min(UN_1, VN_2)\sum_{k=1}^{K}N_{R_k}$ in (16a) and (19).

VII. Impact of practical transmission impairments

In this section, the impact of practical transmission impairments on Tx/Rx antenna selection for MIMO AF TWRNs is studied. Specifically, the detrimental impact of the feedback delays, spatially-correlated fading, and non-identically distributed fading on the system performance is studied by deriving important performance metrics, which provide valuable insights into practical system-designs. Moreover, a channel prediction strategy is proposed and analyzed to mitigate the adverse effect of outdated CSI due to feedback delays.

[12]The corresponding outage probability expression for SS-1 over n.i.i.d. Rayleigh fading can be obtained by replacing N_1 and N_2 by UN_1 and VN_2 in (32).

$$G(z,a,b,c,d)=\sum_{p=0}^{N_1-1}\sum_{q=0}^{N_2-1}N_1N_2\binom{N_1-1}{p}\binom{N_2-1}{q}(-1)^{p+q}\left[\frac{1}{b\hat{\zeta}_{1,p}\hat{\zeta}_{2,q}}\left(\frac{1-\mathrm{e}^{-a\beta z}}{a}-\frac{1-\mathrm{e}^{-(a+b)\beta z}}{a+b}\right)\right.$$
$$\left.-\,c\left(\frac{\mathrm{e}^{-(a+b)\beta z}(1-\mathrm{e}^{-(a+b)\phi(z)})}{a+b}-\frac{\mathrm{e}^{-(a\phi(z)+(a\beta+b\alpha)z)}}{a}\mathcal{J}(z)\right)\right]+\sum_{p=0}^{d-1}(-1)^p\binom{d}{p+1}\mathrm{e}^{-a\beta z}. \quad (24)$$

A. Impact of feedback delays on Tx/Rx antenna selection

In practical wireless systems, antennas selection could be performed by using outdated CSI due to feedback delays. In this subsection, the feedback delay effect on the performance of Tx/Rx antenna selection for MIMO AF TWRNs is studied.

In particular, the feedback channel from the receiver to the transmitter experiences delays. We thus assume that Tx/Rx antennas at S_1, S_2 and R are selected based on the outdated CSI received via the feedback channels of $S_1 \rightarrow R$, and $S_2 \rightarrow R$ having τ_1 and τ_2 time delays, respectively. These two channels can be modeled as [20]

$$\mathbf{H}_{S_iR}(t)\big|_{i=1}^{2}=\rho_i\mathbf{H}_{S_iR}(t-\tau_i)+\mathbf{E}_i, \quad (22)$$

where ρ_i is the normalized correlation coefficients between $h_{S_iR}^{k,l}(t)$ and $h_{S_iR}^{k,l}(t-\tau_i)$. For Clarke's fading spectrum, $\rho_i=\mathcal{J}_0(2\pi f_i\tau_i)$, where f_i is the Doppler fading bandwidth[13]. Further, $\mathbf{E}_i$ is the error matrix incurred by the feedback delay, and is having mean zero and variance $(1-\rho_i^2)$ Gaussian entries.

For the sake of mathematical tractability, we consider single-antenna relays only. Nevertheless, both S_1 and S_2 are equipped with multiple-antennas. Under this channel and system model, the overall outage probability of Tx/Rx antenna selection for MIMO AF TWRNs based on minimizing the overall outage probability is derived as[14] (see Appendix E for the proof)

$$P_{out}=F_Z(\gamma_{th})=G\left(\gamma_{th},\frac{p+1}{\hat{\zeta}_{1,p}},\frac{q+1}{\hat{\zeta}_{2,q}},\frac{1}{(q+1)\hat{\zeta}_{1,p}},N_1\right)$$
$$+\,G\left(\gamma_{th},\frac{q+1}{\hat{\zeta}_{2,q}},\frac{p+1}{\hat{\zeta}_{1,p}},\frac{1}{(p+1)\hat{\zeta}_{2,q}},N_2\right), \quad (23)$$

where the function G is given by (24). In (24), α, ζ, $\phi(z)$, and $\mathcal{J}(z)$ are defined as in (9). Further, $\hat{\zeta}_{1,p}$ and $\hat{\zeta}_{2,q}$ are given by $\hat{\zeta}_{1,p}=\zeta_1\left(1+p(1-\rho_1^2)\right)$ and $\hat{\zeta}_{2,q}=\zeta_2\left(1+q(1-\rho_2^2)\right)$, respectively.

Further insights into the detrimental effect of feedback delays on the performance for antenna selection can be obtained by deriving the asymptotic outage probability at high SNRs as follows (see Appendix E for the proof):

$$P_{out}^{\infty}=\hat{\Omega}\left(\frac{\gamma_{th}}{\bar{\gamma}}\right)+o\left(\bar{\gamma}^{-2}\right), \quad (25a)$$

where $\hat{\Omega}$ is given by

$$\hat{\Omega}=\begin{cases}\left(\frac{C_S+C_R}{C_SC_R}\right)\sum_{q=0}^{N_2-1}\frac{(-1)^qN_2\binom{N_2-1}{q}}{\hat{\zeta}_{2,q}}, & \rho_1=1,0\le\rho_2<1\\ \left(\frac{C_S+C_R}{C_SC_R}\right)\sum_{p=0}^{N_1-1}\frac{(-1)^pN_1\binom{N_1-1}{p}}{\hat{\zeta}_{1,p}}, & \rho_2=1,0\le\rho_1<1\\ \left(\frac{C_S+C_R}{C_SC_R}\right)\left(\sum_{p=0}^{N_1-1}\frac{(-1)^pN_1\binom{N_1-1}{p}}{\hat{\zeta}_{1,p}}\right.\\ \left.+\sum_{q=0}^{N_2-1}\frac{(-1)^qN_2\binom{N_2-1}{q}}{\hat{\zeta}_{2,q}}\right), & 0\le\rho_1<1,0\le\rho_2<1.\end{cases} \quad (25b)$$

By using (25a), the diversity order can be quantified to be unity. Thus, the outdated CSI has a severely detrimental effect on the outage probability, in effect, the achievable diversity order diminishes from $\min(N_1,N_2)$ to one.

B. Channel prediction strategy to circumvent feedback delay effect for Tx/Rx antenna selection

Linear channel prediction can be employed to circumvent outdated CSI due to feedback delays in time varying channels [22], [23]. Thus, in this subsection, such a linear channel prediction strategy is used to minify the adverse effects of feedback delay for Tx/Rx antenna selection in MIMO TWRNs.

For each block-length (L_b symbols of each with symbol duration T_s), the (k,l)th entry of the estimated channel matrix $\hat{H}_{S_iR}(t)\big|_{i=1}^{2}$ is given by

$$\hat{h}_{S_iR}^{k,l}(t)=h_{S_iR}^{k,l}(t)+e_{S_iR}^{k,l}(t),\ \text{ for } i\in\{1,2\}, \quad (26)$$

where $h_{S_iR}^{k,l}(t)$ is the (k,l)th entry of the actual channel matrix $H_{S_iR}(t)\big|_{i=1}^{2}$ and $e_{S_iR}^{k,l}(t)\sim\mathcal{CN}(0,\sigma_{e,i}^2)$ is the Gaussian channel estimation error[15]. Moreover, $h_{S_iR}^{k,l}(t)$ and $e_{S_iR}^{k,l}(t)$ are statistically independent.

By employing classical theory of linear FIR channel prediction [22], [23], the L-block ahead predicted channel entry is derived as[16]

$$\tilde{h}_{S_iR}^{k,l}(t+LL_bT_s)=\mathbf{w}_{\mathrm{opt},i}^H\hat{\mathbf{h}}_{S_iR}^{k,l},\quad \text{for}\quad i\in\{1,2\}, \quad (27)$$

where $\hat{\mathbf{h}}_{S_iR}^{k,l}=[\hat{h}_{S_iR}^{k,l}(t),\hat{h}_{S_iR}^{k,l}(t-L_bT_s),\cdots\hat{h}_{S_iR}^{k,l}(t-(L-1)L_bT_s)]^T$ is the vector of estimated fading amplitudes corresponding to the prediction length L. Further, $\mathbf{w}_{\mathrm{opt},i}^H$ is the optimal weighting vector corresponding to Wiener-Hopf equation [22], [23] and is derived[17] as $\mathbf{w}_{\mathrm{opt}}=\mathbf{R}_i^{-1}\mathbf{r}_i$,

[13]Here, $\mathcal{J}_0(z)$ is the Bessel function of the first kind of order zero [21, Eq. (8.402)].

[14]The impact of outdated CSI due to feedback delays for SS-2 can also be quantified by using similar techniques. However, this result is omitted for the sake of brevity.

[15]Here the channel estimation error variance can be explicitly defined as $\sigma_{e,i}^2=\sigma_i^2/E_p$, where σ_i^2 and E_p are the noise power at each receive antenna and the power of the pilot symbol.

[16]On the contrary to our assumption in Section II, here, a more practical signaling scheme, where each transmission phase is assumed to last L-blocks, is employed. Interestingly, the feedback time delay τ_i defined in (22) can now be defined as $\tau_i=LL_bT_s$.

[17]This optimal weighting vector is derived to minimize the mean square error (MSE) as $\min_{\mathbf{w}_{\mathrm{opt},i}}\sigma_e^2=\sigma_h^2-\mathbf{r}_w^H\mathbf{R}_w^{-1}\mathbf{r}_w$, where σ_e^2 is the predictor error variance [22], [23].

$$F(z,n,N,a,b,\tau,\sigma,\epsilon)=\sum_{p=1}^{N_1}\sum_{q=1}^{N_2}\sum_{\sigma_1}\sum_{\sigma_2}\frac{\text{sign}(\sigma_1)\text{sign}(\sigma_2)}{b\,\zeta_{1,p,m,k}\,\zeta_{2,q,m,k}}\left(\frac{1}{a}\left[1-\text{e}^{-a\beta_k z}\right]-\frac{1}{\mathcal{C}}\left[1-\text{e}^{-\mathcal{C}\beta_k z}\right]\right)+$$
$$\sum_{n=1}^{N}\sum_{\sigma}\sum_{\tau}\text{sign}(\sigma)\text{sign}(\tau)\epsilon\left\{\frac{\text{e}^{-(a+\tau)\beta_k z}\left[1-\text{e}^{-(a+\tau)\phi(z)}\right]}{a+\tau}+\frac{\text{e}^{-[(a\beta_k+\alpha_k\tau)z+a\phi(z)]}}{a}\sum_{t=1}^{T_g}w_t\text{e}^{-\frac{a\tau z(\alpha_k\beta_k z+\eta)}{x_t+a\phi(z)}}\right\},\quad(33)$$

where the (m,n)th entry of $L\times L$ matrix $\mathbf{R}_i$ is given by $[\mathbf{R}_i]_{m,n}=\mathcal{J}_0(2\pi f_i|m-n|L_bT_s)+\sigma^2_{e,i}\delta(m-n)$, and lth entry of $L\times 1$ vector $\mathbf{r}_i$ is given by $[\mathbf{r}_i]_l=\mathcal{J}_0(2\pi f_i|L+l-1|L_bT_s)$.

Next, it can readily be seen that the normalized correlation coefficient between the true and the predicted fading amplitude is given by $\hat{\rho}_i=\sqrt{\mathbf{r}_i^H\mathbf{R}_i^{-1}\mathbf{r}_i}$. Consequently, the (k,l)th entry of the L-block ahead true channel matrix $H_{S_iR}|_{i=1}^2$ can be written as

$$h_{S_iR}^{k,l}=\hat{\rho}_i\,\tilde{h}_{S_iR}^{k,l}+\sqrt{1-\hat{\rho}_i^2}\,n_{S_iR}^{k,l},\quad\text{for}\quad\in\{1,2\},\ (28)$$

where $n_{S_iR}^{k,l}$ is the Gaussian residue error with zero mean and unit variance. It is worth noticing that (22) is in fact the special case of the unit tap form of (28). Thus, the exact overall outage probability and its high SNR approximation of Tx/Rx antenna selection with channel prediction for MIMO TWRNs can be derived by simply replacing ρ_i in (23) and (25a), respectively, by $\hat{\rho}_i=\sqrt{\mathbf{r}_i^H\mathbf{R}_i^{-1}\mathbf{r}_i}$.

C. Impact of spatially-correlated fading

In this subsection, the impact of spatially-correlated fading among multiple antenna elements is studied. To this end, the exact amount of asymptotic performance degradation due to correlated fading is quantified in closed-form. The system model in interest is same as that of Section VII-A and the corresponding channel model is presented as follows:

1) Correlated fading channel model: The channel vector from S_i to the mth antenna at R is assumed to be spatially-correlated flat Rayleigh fading and is given by $\mathbf{\Psi}_i^{\frac{1}{2}}\mathbf{h}_{S_iR}$ for $i\in\{1,2\}$, where $\mathbf{\Psi}_i$ is the $N_i\times N_i$ covariance matrix at S_i and $\mathbf{h}_{S_iR}$ is a $N_i\times 1$ vector with independent Rayleigh fading entries. The (p,q)th element of $\mathbf{\Psi}_i$ for $i\in\{1,2\}$ is given by [24, Eq. (8.1.5)]

$$\mathbf{\Psi}_i^{p,q}=\begin{cases}\rho_{i,p}\rho_{i,q}, & p\neq q\\ 1, & p=q,\end{cases}\quad\text{where}\ \ 0\le(\rho_{i,p},\rho_{i,q})<1.\ (29)$$

Consequently, $\mathbf{\Psi}_i$ can be parameterized by an $1\times N_i$ vector ρ_i with the pth element $\rho_{i,p}$.

2) Asymptotic overall outage probability at high SNRs: The asymptotic overall outage probability at high SNRs for Tx/Rx antenna selection based SS-1 for MIMO TWRNs over correlated Rayleigh fading is derived as (see Appendix F for the proof)

$$P_{out,Corr}^{\infty}=\Omega_{Corr}\left(\frac{\gamma_{th}}{\bar{\gamma}}\right)^{G_{d,Corr}}+o\left(\bar{\gamma}^{-(G_{d,Corr}+1)}\right),\ (30a)$$

where the diversity order is given by

$$G_{d,Corr}=\min(N_1,N_2).\quad(30b)$$

Further, the system dependent coefficient, Ω_{Corr}, is given by

$$\Omega_{Corr}=\begin{cases}\omega_1\left(\frac{C_S+C_R}{\zeta_1C_SC_R}\right)^{N_1}, & N_1<N_2\\ \omega_2\left(\frac{C_S+C_R}{\zeta_2C_SC_R}\right)^{N_2}, & N_1>N_2\\ \left(\omega_1/\zeta_1^N+\omega_2/\zeta_2^N\right)\left(\frac{C_S+C_R}{C_SC_R}\right)^N, & N_1=N_2=N,\end{cases}\quad(30c)$$

where ω_1 and ω_2 are given by

$$\omega_1=\left(\left[1+\sum_{n=1}^{N_1}\frac{\rho_{1,n}}{1-\rho_{1,n}}\right]\prod_{n=1}^{N_1}[1-\rho_{1,n}]\right)^{-1}\quad\text{and}\quad(30d)$$

$$\omega_2=\left(\left[1+\sum_{n=1}^{N_2}\frac{\rho_{2,n}}{1-\rho_{2,n}}\right]\prod_{n=1}^{N_2}[1-\rho_{2,n}]\right)^{-1}.\quad(30e)$$

3) Amount of performance degradation due to correlated fading: In this subsection, the amount of performance degradation due to correlated fading is quantified analytically. It is worth noticing that the achievable diversity order (30b) of Tx/Rx antenna selection for MIMO TWRNs remains the same even over the correlated Rayleigh fading. However, the array gain is severely affected. In this context, the asymptotic average transmit SNR gap at high SNRs ($\bar{\gamma}_{\text{gap}}^{\infty}$), which is defined as the ratio of the average transmit SNRs of uncorrelated and correlated cases at a fixed outage probability for a given threshold SNR, is derived as

$$\bar{\gamma}_{\text{gap}}^{\infty}=\begin{cases}(\omega_1)^{-1/G_d}, & N_1<N_2\\ (\omega_2)^{-1/G_d}, & N_1>N_2\\ \left[\left(\zeta_1^N+\zeta_2^N\right)/\left(\zeta_1^N\omega_2+\zeta_2^N\omega_1\right)\right]^{-1/G_d}, & N_1=N_2=N.\end{cases}\quad(31)$$

It is worth noticing that $\bar{\gamma}_{\text{gap}}^{\infty}$ can now be used to design the required fade-margins to countermeasure the SNR loss due to spatially-correlated fading in practical MIMO TWRNs set-ups.

D. Impact of non-identically distributed fading

In this subsection, the effect of non-identically and independently distributed (n.i.i.d.) Rayleigh fading on the performance of joint relay and Tx/Rx antenna selection is investigated. To this end, the overall outage probability of joint relay and Tx/Rx antenna selection based on SS-1 for MIMO AF two-way multi-relay networks over n.i.i.d. Rayleigh fading is derived as (see Appendix G for the proof).

$$P_{out}=\prod_{k=1}^{K}\prod_{m=1}^{N_{R_k}}\left(\mathcal{A}_{k,m}+\mathcal{B}_{k,m}\right),\quad(32)$$

where $\mathcal{A}_{k,m}$ and $\mathcal{B}_{k,m}$ are given by

$$\mathcal{A}_{k,m}=F\left(\gamma_{th},p,N_1,\sigma_1+\zeta_{1,p,m,k}^{-1},\sigma_2+\zeta_{2,q,m,k}^{-1},\tau_2,\sigma_1,\zeta_{1,p,m,k}^{-1}\right),$$
$$\mathcal{B}_{k,m}=F\left(\gamma_{th},q,N_2,\sigma_2+\zeta_{2,q,m,k}^{-1},\sigma_1+\zeta_{1,p,m,k}^{-1},\tau_1,\sigma_2,\zeta_{2,q,m,k}^{-1}\right).$$

In (32), the function $F(z,n,N,a,b,c,d,\epsilon)$ is defined as (33). Further, in (33), the variables $\mathcal{C}$, σ_i and τ_i for $i\in\{1,2\}$ are defined as $\mathcal{C}=\sigma_1+\sigma_2+\frac{\zeta_{1,p,m,k}+\zeta_{2,q,m,k}}{\zeta_{1,p,m,k}\zeta_{2,q,m,k}}$, $\sigma_1\in\mathcal{S}_{p,u,k}^{N_1}$,

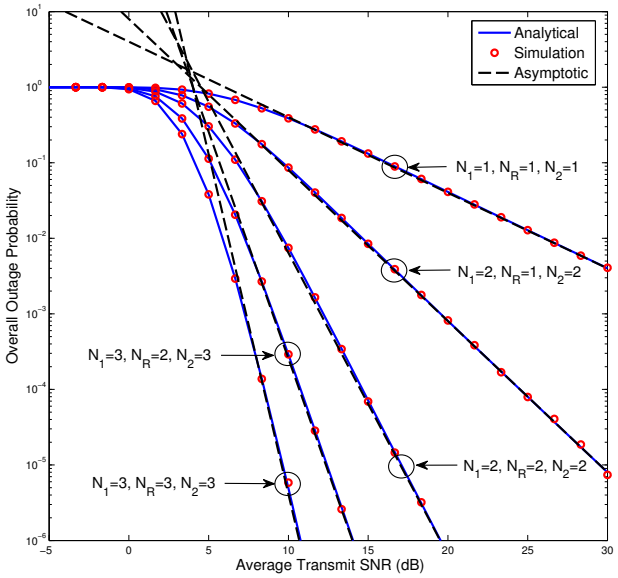

Fig. 2. The overall outage probability of Tx/Rx antenna selection strategy based on minimizing the outage probability for a MIMO AF TWRN with a single relay. The target rate of the whole system is R_{th} = 2 bits/Hz/s. Since the two source nodes are identical, their individual target rates are considered as $\frac{R_{th}}{2}$. The hop distances are $d_{S_1R} = d_{S_2R}$ and the path-loss exponent is $\varpi = 3.5$.

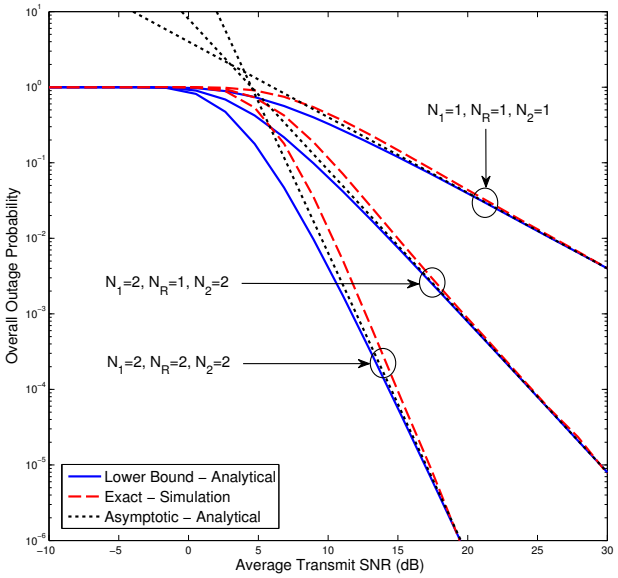

Fig. 3. The overall outage probability of Tx/Rx antenna selection based on the maximization of the sum-rate. The target sum-rate of the whole system is R_{th} = 2 bits/Hz/s. The hop distances are $d_{S_1R} = d_{S_2R}$ and the path-loss exponent is $\varpi = 3.5$.

$\sigma_2 \in \mathcal{S}_{q,v,k}^{N_2}$, $\tau_1 \in \mathcal{T}_{p,k}^{N_1}$, and $\tau_2 \in \mathcal{T}_{q,k}^{N_2}$, respectively. Moreover, the sets $\mathcal{S}_{a,b,k}^{N_i}$ and $\mathcal{T}_{a,k}^{N_i}$ are defined as [25]

$$\mathcal{S}_{a,b,c}^{N_i} = \left\{ \sigma_i : \prod_{a=1, b\neq a}^{N_i} \left(1 - \mathrm{e}^{-\frac{x}{\zeta_{i,a,m,k}}}\right) = \sum_{\sigma_i \in \mathcal{S}_{a,b,c}^{N_i}} \mathrm{sign}(\sigma_i) \mathrm{e}^{-\sigma_i x} \right\}, \quad (34)$$

$$\mathcal{T}_{a,k}^{N_i} = \left\{ \tau_i : \prod_{a=1}^{N_i} \left(1 - \mathrm{e}^{-\frac{x}{\zeta_{i,a,m,k}}}\right) = \sum_{\tau_i \in \mathcal{T}_{a,k}^{N_i}} \mathrm{sign}(\tau_i) \mathrm{e}^{-\tau_i x} \right\}. \quad (35)$$

where $\mathrm{sign}(\sigma_i)$ and $\mathrm{sign}(\tau_i)$ correspond to the sign of each term in the expansion of the product terms. The corresponding asymptotic high SNR approximation of the overall outage probability (32) can readily be obtained by replacing Ω_k in (16a) by

$$\Omega_k' = \begin{cases} \left(\frac{C_S + C_R}{C_S C_R}\right)^{N_1 N_{R_k}} \prod_{m=1}^{N_{R_k}} \prod_{p=1}^{N_1} \zeta_{1,p,m,k}^{-1}, & N_1 < N_2 \\ \left(\frac{C_S + C_R}{C_S C_R}\right)^{N_2 N_{R_k}} \prod_{m=1}^{N_{R_k}} \prod_{q=1}^{N_2} \zeta_{2,q,m,k}^{-1}, & N_1 > N_2 \\ \left(\frac{C_S + C_R}{C_S C_R}\right)^{N N_{R_k}} \prod_{m=1}^{N_{R_k}} \left(\prod_{p=1}^{N_1} \zeta_{1,p,m,k}^{-1} \right. & \\ \left. + \prod_{q=1}^{N_2} \zeta_{1,q,m,k}^{-1} \right), & N_1 = N_2 = N. \end{cases} \quad (36)$$

VIII. Numerical Results

This section presents the numerical results and Monte-Carlo simulations for the performance of the proposed Tx/Rx antenna selection strategies.

A. Outage probability of MIMO AF single-relay TWRNs based on SS-1 and SS-2

Fig. 2 shows the overall outage probability of the Tx/Rx antenna selection strategy based on minimizing the outage probability (SS-1) for single-relay MIMO AF TWRNs. The analytical outage curves are plotted for several antenna set-ups by using (8) and (12a). In particular, the outage curve corresponding to the single-antenna TWRN is plotted as a benchmark. Fig. 2 clearly reveals that the multi-antenna TWRNs with SS-1 provide significant gains over the single-antenna TWRNs. In fact, at 10^{-2} outage probability, the triple-antenna TWRN provides a 20.34 dB gain over the single-antenna TWRN. The asymptotic outage curves, which are exact at high SNRs, clearly reveal the diversity order of the system and provide insights into practical two-way relay system designing. The exact match between Monte-Carlo simulations and analytical curves verifies the accuracy of our derivations.

Similarly, Fig. 3 shows the outage probability of the Tx/Rx antenna selection strategy based on maximizing the sum-rate (SS-2) for single-antenna MIMO AF TWRNs. The exact outage curves are Monte-Carlo simulations whereas the lower bounds and the asymptotic curves are plotted by using (11) and (19), respectively. Fig. 3 clearly reveals the performance gains of the Tx/Rx antenna selection for multi-antenna TWRNs over the single-antenna TWRNs. The outage probability lower bound in (11) is asymptotically exact, and hence, the high SNR approximation of the outage probability yields this asymptotic exactness. Thus, our bounds and approximations provide an accurate assessment of the system performance and, hence, are useful as benchmarks for practical system designing.

B. Outage probability of joint relay and Tx/Rx antenna selection for MIMO AF multi-relay TWRNs

In Fig. 4, the overall outage probability of multi-relay MIMO AF TWRNs with a common antenna configuration (i.e., $N_1 = 2, N_R = 2, N_2 = 2$) is plotted for several relay set-ups. Specifically, the Tx/Rx antenna selection is performed

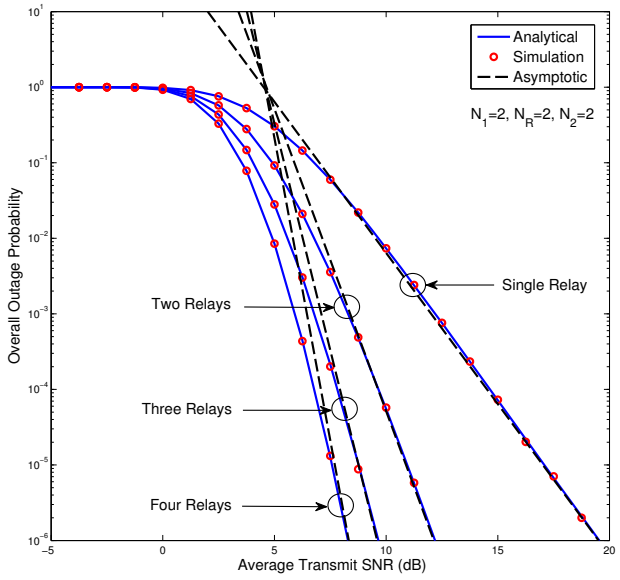

Fig. 4. The overall outage probability of joint relay and Tx/Rx antenna selection for MIMO AF TWRNs based on the minimizing the outage probability. The target rate of the whole system and individual sources are 2 bits/Hz/s and 1 bits/Hz/s, respectively. The hop distances are $d_{S_1R} = d_{S_2R}$ and the path-loss exponent is $\varpi = 3.5$.

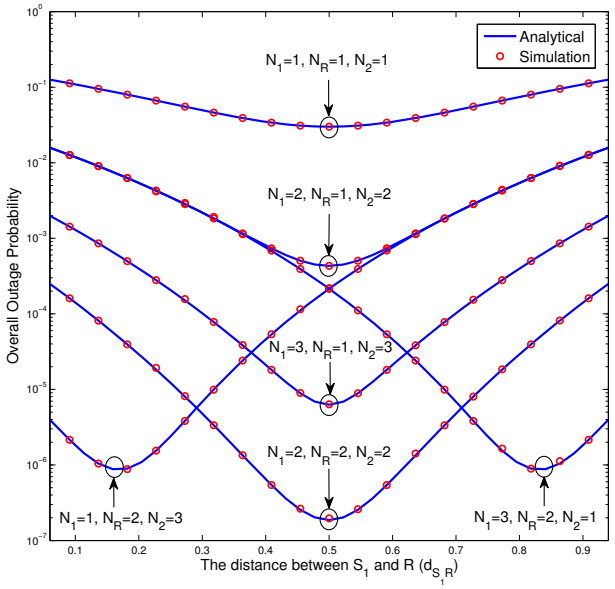

Fig. 5. The overall outage probability of verses the relay location. Here, ζ_1 and ζ_2 are modeled as $\zeta_1 = (d_{S_1R})^{-\varpi}$ and $\zeta_2 = (d_{S_2R})^{-\varpi}$, where $\varpi = 3.5$. The transmit SNRs at each terminal is 10.79 dB. The target rate of the whole system and individual sources are 2.5 bits/Hz/s and 1.25 bits/Hz/s, respectively.

based on minimizing the overall outage probability (SS-1)[18]. The analytical curves are plotted by using (15) and (16a). The outage curves corresponding to the single-relay TWRN is plotted as a benchmark. Fig. 4 clearly illustrates the performance gains of joint relay and Tx/Rx antenna selection of the multi-relay TWRNs over that of their single-relay counterpart. For example, at 10^{-5} outage probability, the quadruple-relay TWRN provides a gain of 9.5 dB over that of its single-relay counterpart. Further, the asymptotic outage curves verify our diversity order analysis. Monte-Carlo simulations agree exactly with analytical outage curves, validating our analysis.

C. The effect of relay location on the outage probability

In Fig. 5, the effect of the relay location on the overall outage probability for SS-1 is studied[19]. Specifically, the outage probability is plotted against the distance between S_1 and R by modeling the path-loss dependent parameters ζ_1 and ζ_2 in (8) and (15) as $\zeta_1 = (d_{S_1R})^{-\varpi}$ and $\zeta_2 = (d_{S_2R})^{-\varpi}$ where $\varpi = 3.5$ is the path-loss exponent. Here, d_{S_1R} and d_{S_1R} are the distances between $S_1 \rightarrow R$ and $S_2 \rightarrow R$, respectively and they satisfy $d_{S_1R} + d_{S_1R} = 1$. Fig. 5 provides the following valuable insights: (i) when the antenna configuration at S_1, R and S_2 is symmetric (i.e., $N_1 = N$, $N_R = M$, $N_2 = N$), the optimal relay location, which minimizes the overall outage probability, is the half-way point between S_1 and S_2, and (ii) when the antenna configuration at each terminal is asymmetric, this optimal relay location shifts toward the source, which has the lowest number of antennas.

[18]The outage probability curves of the joint relay and Tx/Rx antenna selection based on maximizing the sum-rate behave similarly to those of Fig. 4 and, hence, are omitted for the sake of brevity.

[19]The effect of the relay location on the outage probability for SS-2 shows similar trends to those of $SS-1$ in Fig. 5, and hence, is omitted for the sake of brevity.

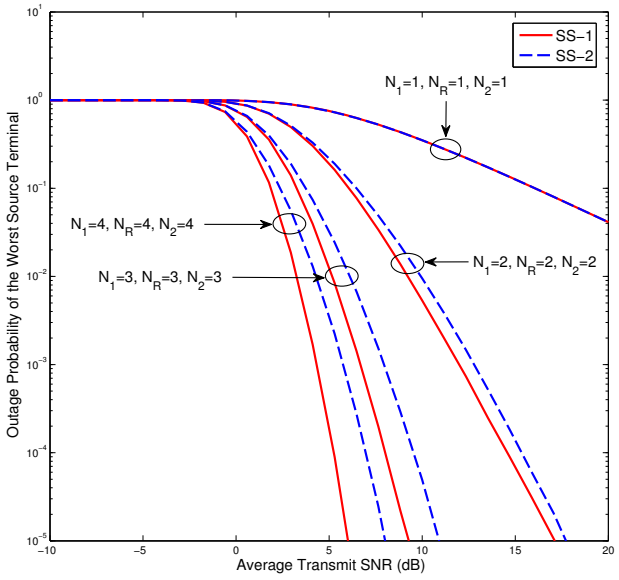

Fig. 6. The comparison of the overall outage probability of Tx/Rx antenna selection based on the two proposed design criteria i.e., (i) minimizing the outage probability and (ii) maximizing the sum-rate. The target sum-rate of the whole system is R_{th} = 2 bits/Hz/s and the target rate of both S_1 and S_2 is 1 bits/Hz/s. The hop distances are $d_{S_1R} = 0.20\, d_{S_2R}$ and the path-loss exponent is $\varpi = 3.5$.

D. Comparison of the outage probability of SS-1 and SS-2

Fig. 6 compares the outage probability of two Tx/Rx selection strategies; (i) minimizing the overall outage probability (SS-1) and (ii) maximizing the sum-rate (SS-2) defined in (4) and (6), respectively. Specifically, the outage probability of the worst source terminal, which has the lowest end-to-end SNR, is plotted for several antenna set-ups by using Monte-Carlo simulations. Here, the relay node is situated in an asymmetric

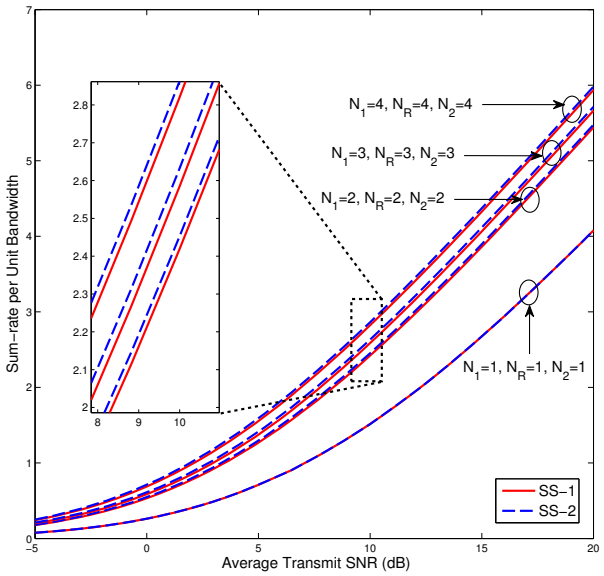

Fig. 7. The comparison of the average sum-rate of Tx/Rx antenna selection based on the two proposed design criteria i.e., (i) minimizing the outage probability (SS-1) and (ii) maximizing the sum-rate (SS-2). The hop distances are $d_{S_1R} = 1.25\, d_{S_2R}$ and the path-loss exponent is $\varpi = 4.0$.

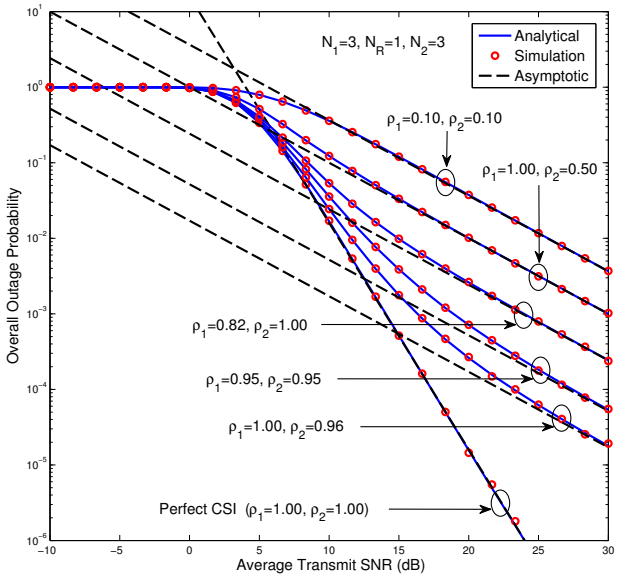

Fig. 8. The feedback delay effect on the outage probability of Tx/Rx antenna selection based on minimizing the outage probability (SS-1). The hop distances are $d_{S_1R} = d_{S_2R}$ and the path-loss exponent is $\varpi = 3.5$.

position between two sources, i.e., $d_{S_1R} = 0.20\, d_{S_2R}$. Fig. 6 clearly reveals that both selection strategies perform equally well in terms of the outage probability for lower number of antennas at each terminals. However, as the number of antennas at each terminal increases, SS-1 outperforms SS-2 in terms of the outage probability. For example, at 10^{-4} outage probability, SS-1 achieves about 1.5 dB SNR gain over SS-2. This behavior is expected as SS-1 is designed to maximize the e2e SNR of the worst source terminal, and hence, to minimize the overall outage probability.

E. Comparison of the average sum-rate of SS-1 and SS-2

Similarly, Fig. 7 compares the average sum-rate of two Tx/Rx selection strategies, SS-1 and SS-2 in (4) and (6), respectively. Several average sum-rate curves are plotted against the average transmit SNR by using Monte-Carlo simulations. Specifically, several antenna set-ups are used to compare the effect of the number of Tx/Rx antennas on the average sum-rate by locating the relay in a slightly asymmetric position between two sources as $d_{S_1R} = 1.25\, d_{S_2R}$. Both selection strategies perform equally well for each antenna set-up. Nevertheless, when the number of antennas at each terminal increases, SS-2 slightly outperforms SS-1 in terms of the average sum-rate as depicted in the magnified portion of the figure. This behavior is expected as SS-2 is designed to maximize the sum-rate of the whole system. Moreover, Fig. 7 and Fig. 6 provide the important insight that the both selection strategies perform almost identically in terms of the outage probability and the average sum-rate whenever the relay is located symmetrically between two sources, however, this performance gap increases whenever the relay is positioned asymmetrically.

F. Impact of feedback delays on the outage probability of SS-1

Fig. 8 shows the impact of feedback delays on the outage probability for Tx/Rx antenna pair selection of SS-1 by considering a MIMO AF TWRN with $N_1 = 3$, $N_R = 1$ and $N_2 = 3$. The outage probability is plotted for several feedback delay scenarios by changing ρ_1 and ρ_2. The outage curve with $\rho_1 = \rho_2 = 1$ corresponds to the perfect CSI case (i.e., antenna selection with perfect CSI) whereas the curve with $0 \leq \rho_1, \rho_2 < 1$ corresponds to the imperfect CSI case. As ρ_1 and ρ_2 decrease from 1 to 0 (i.e., as the feedback delay increases), the performance of Tx/Rx antenna selection degrades significantly. In particular, Fig. 8 shows that even a slight feedback delay in either hop results in severe degradation of the diversity order. This result is clearly revealed by the curves corresponding to $(\rho_1 = 1,\ \rho_2 = 0.95)$ and $(\rho_1 = 0.82,\ \rho_2 = 1)$, respectively, where one hop has no feedback delays, and the other hop has a slight feedback delay. Specifically, our asymptotic analysis clearly reveals that the Tx/Rx antenna selection based on the perfect CSI achieves the full diversity available in the MIMO two-way relay channel; $G_d = \min(N_1, N_2)$. However, when the antennas are selected based on the outdated CSI, this diversity gain decreases to one. Specifically, at 10^{-3} outage probability, a 15.76 dB performance loss is incurred when the antenna selection is based on CSI related to $\rho_1 = 1$ and $\rho_2 = 0.5$ over the perfect CSI case. The exact match between the Monte-Carlo simulation points and the analytical results verifies the accuracy of our analysis.

G. Channel prediction to circumvent feedback delay effect

In Fig. 9, the effect of linear channel prediction to circumvent detrimental impact of outdated CSI due to feedback delay for Tx/Rx antenna selection based on SS-1 is studied for a MIMO TWRN with $(N_1 = 3,\ N_R = 1,\ N_2 = 3)$ antenna configuration. A set of outage curves are plotted by

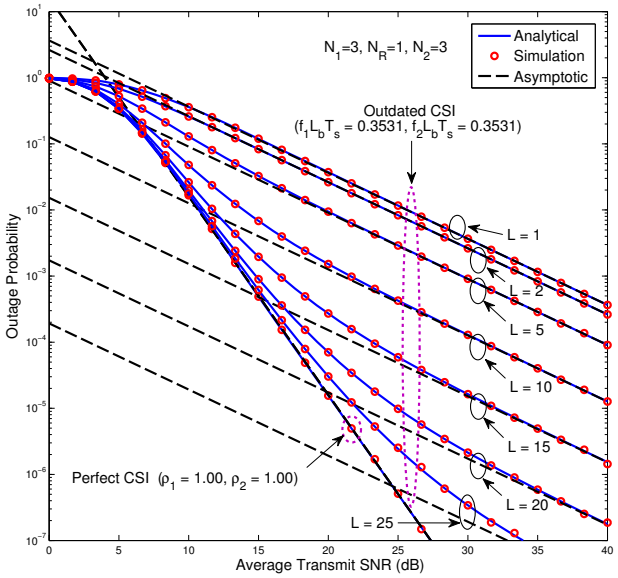

Fig. 9. Channel prediction to circumvent the feedback delay effect on the outage probability of Tx/Rx antenna selection based on minimizing the outage probability (SS-1). The FIR channel predictor length for each individual hop is denoted by L. The hop distances are $d_{S_1R} = d_{S_2R}$ and the path-loss exponent is $\varpi = 3.5$.

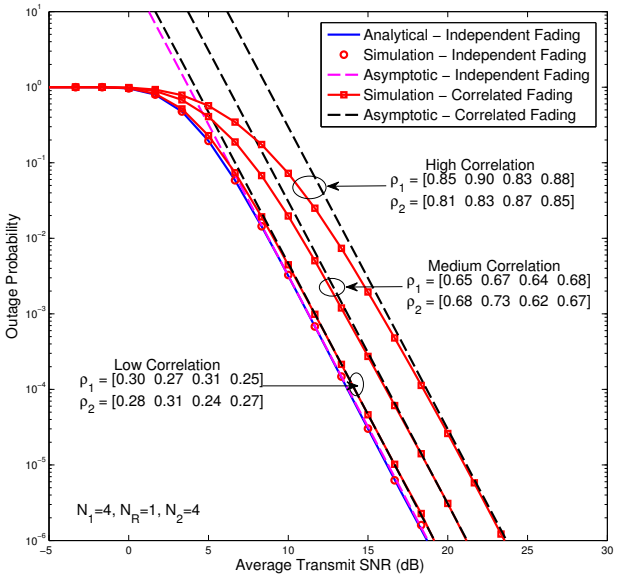

Fig. 10. Impact of correlated fading on the outage probability of Tx/Rx antenna selection based on minimizing the outage probability (SS-1). The hop distances are $d_{S_1R} = d_{S_2R}$ and the path-loss exponent is $\varpi = 3.5$.

varying the the FIR channel predictor length L. Our results clearly reveal that a significant performance improvement can be obtained by increasing the predictor length. For example, at 10^{-3} outage probability, a FIR predictor with 20 taps provides almost 21 dB SNR gain over a single-tap predictor. It is also worth noticing that the diversity order loss can not be recovered completely by FIR linear prediction. However, a significant fraction of outage probability loss resulted from the outdated CSI can be recovered by using causal FIR prediction. For instance, at 10^{-5} outage probability, a 25 tap FIR predictor only looses 1.3 dB compared to the perfect CSI case. Intuitively, it can be concluded that an infinite impulse response (IIR) predictor would fully recover the diversity order loss resulted from feedback delay effect.

H. Impact of correlated fading

Fig. 10 shows the impact of correlated fading on the overall outage probability of Tx/Rx antenna selection based on SS-1 for a MIMO TWRN with $(N_1 = 4, N_R = 1, N_2 = 4)$ antenna setup. Four specific spatial correlation effects are considered as (i) independent fading (ii) low correlation, (iii) medium correlation and (iv) high correlation by varying relative antenna spacing, angle of arrival/departure and angular spread. Our asymptotic outage curves clearly reveal that the spatial correlation degrades the outage probability significantly. It is also worth noticing that while spatial correlation does not degrade the achievable diversity order, it does degrade the array gain. For instance, at 10^{-5} outage probability, high correlation results in almost 5 dB outage loss with respective to independent fading case. This asymptotic outage loss agrees well with our analytical results presented in Section VII-C, and hence render themselves useful for obtaining valuable insights into practical MIMO TWRN system designing.

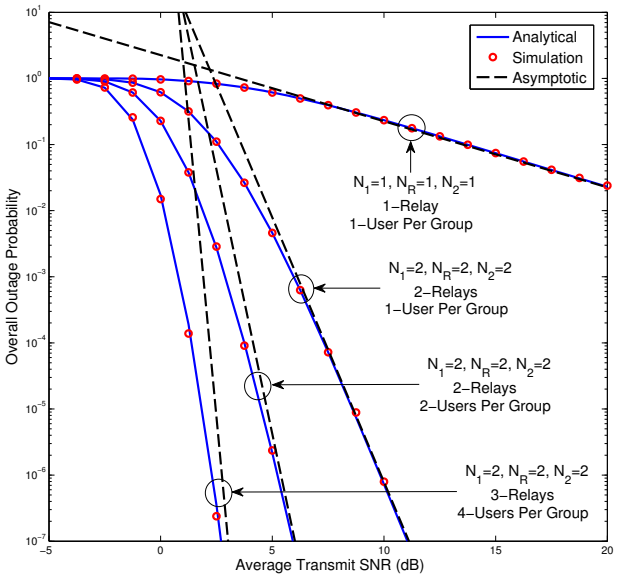

Fig. 11. The overall outage probability of joint user, relay and antenna selection based on (SS-1) for MIMO multi-user/multi-relay TWRNs over n.i.i.d. fading. The n.i.i.d. fading parameter $\zeta_{i,p,m,u}$, $i \in \{1, 2\}$, $p \in \{1 \cdots N_i\}$, $m \in \{1 \cdots N_R\}$ and $u_i \in \{1 \cdots U_i\}$ are defined as $\zeta_{i,p,m,u} = (d_{S_{i,u}R_m})^{-\varpi_{i,m,u}}$. Further, $d_{S_{1,u}R_m} = 1.5\, d_{S_{2,u}R_m}$ and $\varpi_{2,m,u} = 0.75\, \varpi_{1,m,u}$.

I. Multi-user MIMO TWRNs over n.i.i.d. Rayleigh fading

In Fig. 11, the overall outage probability is plotted for the joint user, relay and antenna selection based on SS-1 for MIMO multi-user multi-relay TWRNs over n.i.i.d. Rayleigh fading. Our results clearly reveal that the joint user, relay and antenna selection provides significant outage probability gains over the single-antenna single-user pair counterparts. Specifically, at 10^{-5} outage probability, a SNR gain of 4.1 dB can be obtained by going from the single-user pair configuration to the dual-user pair configuration for the dual-antenna dual-

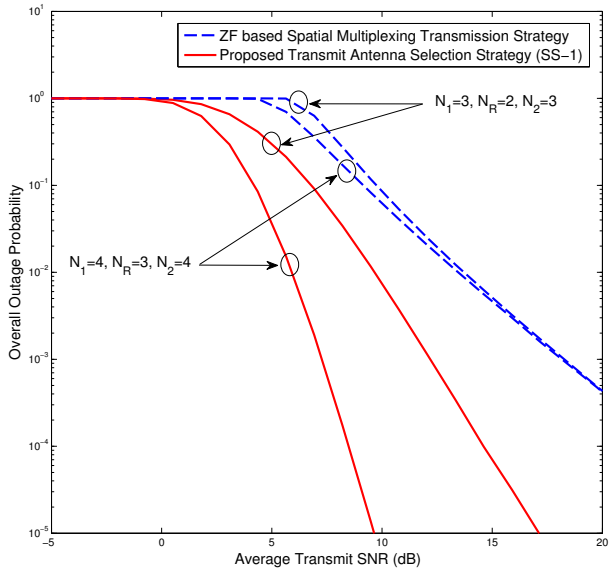

(a) Outage probability Comparison

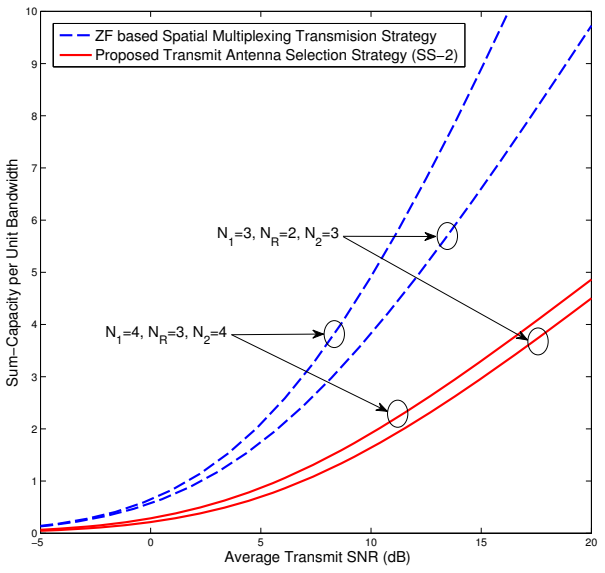

(b) Sum-rate Comparison

Fig. 12. Performance comparison of Tx/Rx antenna selection versus zero-forcing based spatial multiplexing transmission strategy for MIMO AF TWRNs. The hop distances are $d_{S_1R} = 2d_{S_2R}$ and the path-loss exponent is $\varpi = 4.1$.

relay MIMO TWRN. Moreover, our analytical outage curves agrees well with the simulation points, and thus, verifying our analysis in (32) and (36).

J. Performance comparison: Antenna selection vs zero-forcing based spatial multiplexing transmission

In Fig. 12, the performance of the proposed Tx/RX antenna selection versus zero-forcing based spatial multiplexing (ZF-SM) transmission strategy [26] for MIMO TWRNs is compared in terms of the outage probability and average sum-rate. Specifically, the former transmission strategy employs only one antenna/RF chain at each terminal, whereas the latter strategy employs all available antenna/RF chains. Interestingly, as per Fig. 12a, the proposed antenna selection strategy based on SS-1 significantly outperforms the ZF-SM strategy in terms of the overall outage probability. Moreover, the achievable diversity order of antenna selection is considerably higher than that of the ZF-SM. On the other hand, according to Fig. 12b, the ZF-SM achieves significant performance gains over antenna selection based on SS-2 in terms of the average sum-rate. In fact, the average sum-rate of ZF-SM increases linearly with the number of antennas at the relay. The behaviors of Fig. 12a and Fig. 12b are resulted from fundamental diversity-multiplexing trade-off (DMT) of wireless systems. In this context, the DMTs of the proposed antenna selection strategy and ZF-SM [26] can be quantified as $d_{\text{AS}}(r) = N_R \min(N_1, N_2)\,(1-r)$ and $d_{\text{ZF-SM}}(r) = (\min(N_1, N_2) - N_R + 1)\left(1 - \frac{r}{N_R}\right)$, respectively.

IX. Conclusion

Two new Tx/Rx antenna selection strategies were proposed and analyzed for MIMO AF TWRNs based on (i) the minimization of the overall outage probability and (ii) the maximization of the sum-rate. The performance of these strategies was quantified by deriving the overall outage probability. Specifically, the diversity orders were derived by using the high SNR approximations of the outage probability. In particular, we treated the multi-relay, and multi-relay/multi-user generalizations of MIMO AF TWRNs by proposing and analyzing the corresponding joint relay and Tx/Rx antenna selection strategies. The detrimental effects of three practical transmission impairments; (i) feedback delays, (ii) spatially-correlated fading, and (iii) n.i.i.d. fading are quantified to obtain useful insights into practical TWRN system-design. Moreover, linear FIR channel prediction was studied to circumvent the adverse effects of outdated CSI. Numerical results were provided to show the system performance, and thereby, to obtain valuable insights into practical two-way MIMO relay system designing. Notably, our proposed selection strategies are optimal in the sense of outage probability, and hence, in the sense of diversity order as well. Importantly, the joint relay and antenna selection strategies improve the diversity gains over the single-relay counterparts by a factor equal to the total number of all available antennas at the relays. In fact, these strategies achieve full diversity gains while minimizing the cost of implementing multiple Tx/Rx RF chains.

Appendix A
Proof of the CDF of the effective e2e SNR of SS-1

$$F_Z(z) = \Pr\left[Z = \max_{\substack{1\le j\le N_1, 1\le l\le N_2 \\ 1\le m\le N_R}} \left\{\min\left(\gamma_{S_1}^{(j,l,m)}, \gamma_{S_2}^{(j,l,m)}\right)\right\} \le z\right]$$
$$= \Pr\left[\max_{1\le m\le N_R} \left\{\min\left(\gamma_{S_1}^{(J,L,m)}, \gamma_{S_2}^{(J,L,m)}\right)\right\} \le z\right], \qquad (37)$$

$$P_1(z) = \Pr\left[\{X_m \le \beta z\} \cap \{Y_m \le X_m\}\right] + \Pr\left[\left\{Y_m \le \frac{z(\alpha X_m + \eta)}{X_m - \beta z}\right\} \cap \{Y_m \le X_m\}\right]$$
$$= \underbrace{\int_{x=0}^{\beta z}\int_{y=0}^{x} f_{X_m}(x)\, f_{Y_m}(y)\,\mathrm{d}y\mathrm{d}x}_{\mathcal{I}_1(z)} + \underbrace{\int_{t=0}^{\infty} \Pr\left[Y_m \le \min\left(\frac{z(\alpha(t+\beta z)+\eta)}{t}, t+\beta z\right)\right] f_{X_m}(t+\beta z)\,\mathrm{d}t}_{\mathcal{I}_1'(z)}. \quad (41)$$

$$\mathcal{I}_1'(z) = \underbrace{\int_{t=0}^{\phi(z)} F_{Y_m}(t+\beta z)\, f_{X_m}(t+\beta z)\,\mathrm{d}t}_{\mathcal{I}_2(z)} + \underbrace{\int_{t=\phi(z)}^{\infty} F_{Y_m}\left(\frac{z(\alpha(t+\beta z)+\eta)}{t}\right) f_{X_m}(t+\beta z)\,\mathrm{d}t}_{\mathcal{I}_3(z)}. \quad (43)$$

where $\gamma_{S_1}^{(j,l,m)}$ and $\gamma_{S_2}^{(j,l,m)}$ are defined in (3). Further, $\gamma_{S_2}^{(J,L,m)}$ and $\gamma_{S_2}^{(J,L,m)}$ are given by

$$\gamma_{S_1}^{(J,L,m)} = \max_{1\le j\le N_1, 1\le l\le N_2}\left(\gamma_{S_1}^{(j,l,m)}\right) = \frac{X_m Y_m}{\alpha X_m + \beta Y_m + \eta} \text{ and}$$
$$\gamma_{S_2}^{(J,L,m)} = \max_{1\le j\le N_1, 1\le l\le N_2}\left(\gamma_{S_2}^{(j,l,m)}\right) = \frac{X_m Y_m}{\beta X_m + \alpha Y_m + \eta}, \quad (38)$$

where $X_m = |h_{S_1R}^{(m,J)}|^2 = \max_{1\le j\le N_1}\left(|h_{S_1R}^{(m,j)}|^2\right)$, and $Y_m = |h_{S_2R}^{(m,L)}|^2 = \max_{1\le l\le N_2}\left(|h_{S_2R}^{(m,l)}|^2\right)$. Here, $\alpha = \frac{\bar\gamma_S + \bar\gamma_R}{\bar\gamma_S \bar\gamma_R}$, $\beta = \frac{1}{\bar\gamma_R}$ and $\eta = \frac{1}{\bar\gamma_S \bar\gamma_R}$, where $\bar\gamma_S = \frac{\mathcal{P}_S}{\sigma_S^2}$ and $\bar\gamma_R = \frac{\mathcal{P}_R}{\sigma_R^2}$ are the average transmit SNRs at the source nodes and the relay[20].

Now, we define $Z_m = \min\left(\gamma_{S_1}^{(J,L,m)}, \gamma_{S_2}^{(J,L,m)}\right)$ and simplify it as follows[21]:

$$Z_m = \begin{cases} \gamma_{S_1}^{(J,L,m)}, & Y_m \le X_m \\ \gamma_{S_2}^{(J,L,m)}, & Y_m > X_m. \end{cases} \quad (39)$$

Next, the CDF of Z_m can be derived as

$$F_{Z_m}(z) = \Pr[Z_m \le z] = P_1(z) + P_2(z), \quad (40a)$$

where $P_1(z)$ and $P_2(z)$ are given by

$$P_1(z) = \Pr\left[\left\{\gamma_{S_1}^{(J,L,m)} \le z\right\} \cap \{Y_m \le X_m\}\right] \text{ and} \quad (40b)$$

$$P_2(z) = \Pr\left[\left\{\gamma_{S_2}^{(J,L,m)} \le z\right\} \cap \{X_m < Y_m\}\right]. \quad (40c)$$

After some manipulations, the probability $P_1(z)$ can be expressed in a more mathematically tractable form as (41). The $\min(\cdot,\cdot)$ in $\mathcal{I}_1'(z)$ can be simplified as

$$\min\left(\frac{z(\alpha(t+\beta z)+\eta)}{t}, t+\beta z\right) = \begin{cases} t+\beta z, & 0 \le t \le \phi(z) \\ \frac{z}{t}\left[\alpha(t+\beta z)+\eta\right], & t \ge \phi(z), \end{cases} \quad (42)$$

where $\phi(z)$ is derived by solving the quadratic equation $t^2 + (\beta-\alpha)zt - z(\alpha\beta z + \eta) = 0$, and taking the viable root as $\phi(z) = 0.5(\alpha-\beta)z + 0.5\sqrt{(\alpha-\beta)^2 z^2 + 4z(\alpha\beta z + \eta)}$. Consequently, $\mathcal{I}_1'(z)$ can be simplified as in (43).

Next, $P_1(z)$ in (40b) is derived as

$$P_1(z) = \mathcal{I}_1(z) + \mathcal{I}_2(z) + \mathcal{I}_3(z). \quad (44)$$

In (41), $F_{X_m}(x)$ and $F_{Y_m}(y)$ are the CDFs of X_m and Y_m (38), respectively, and given by [27]

$$F_{X_m}(x) = \left[F_{|h^{(m,j)}|^2}(x)\right]^{N_1} = \sum_{p=0}^{N_1}\binom{N_1}{p}(-1)^p \mathrm{e}^{-\frac{px}{\zeta_1}} \text{ and}$$
$$F_{Y_m}(y) = \left[F_{|h^{(m,l)}|^2}(y)\right]^{N_2} = \sum_{q=0}^{N_2}\binom{N_2}{q}(-1)^q \mathrm{e}^{-\frac{qy}{\zeta_2}}. \quad (45)$$

Moreover, $f_{X_m}(x)$ and $f_{Y_m}(y)$ are the PDFs of X_m and Y_m, respectively, and given by

$$f_{X_m}(x) = \sum_{p=0}^{N_1-1}\frac{N_1\binom{N_1}{p}(-1)^p}{\zeta_1}\mathrm{e}^{-\frac{(p+1)x}{\zeta_1}} \text{ and}$$
$$f_{Y_m}(y) = \sum_{q=0}^{N_2-1}\frac{N_2\binom{N_2}{q}(-1)^q}{\zeta_2}\mathrm{e}^{-\frac{(q+1)y}{\zeta_2}}. \quad (46)$$

By substituting (45) and (46) into (41), $\mathcal{I}_1(z)$ and $\mathcal{I}_2(z)$ can be evaluated exactly in closed-form as given in the first and second terms of (9). Specifically, $\mathcal{I}_3(z)$ is too mathematically intractable to be exactly solved, and thus, two efficient evaluation techniques are provided as follows:

A. By using GLQ [18, Eq. (25. 4. 45)]

The integral $\mathcal{I}_3$ is given by

$$\mathcal{I}_3(z) = \sum_{p=0}^{N_1-1}\sum_{q=0}^{N_2}\frac{N_1\binom{N_1-1}{p}\binom{N_2}{q}(-1)^{p+q}}{\zeta_1}\mathrm{e}^{-z\left(\frac{(p+1)\beta}{\zeta_1}+\frac{q\alpha}{\zeta_2}\right)} \times \int_{\phi(z)}^{\infty}\mathrm{e}^{-\left(\frac{(p+1)t}{\zeta_1}+\frac{pz(\alpha\beta z+\eta)}{\zeta_2 t}\right)}\mathrm{d}t, \quad (47a)$$

where α, β, η, and $\phi(z)$ are defined in (9). Now, (47a) is re-arranged to obtain GLQ form as

$$\mathcal{I}_3(z) = \sum_{p=0}^{N_1-1}\sum_{q=0}^{N_2}\frac{N_1\binom{N_1-1}{p}\binom{N_2}{q}(-1)^{p+q}}{p+1} \times \mathrm{e}^{-\left[z\left(\frac{(p+1)\beta}{\zeta_1}+\frac{q\alpha}{\zeta_2}\right)+\frac{(p+1)\phi(z)}{\zeta_1}\right]}\int_0^{\infty}\Psi(x)\mathrm{e}^{-x}\mathrm{d}x, \quad (47b)$$

[20] Without loss of generality, the transmit powers and the AWGN noise variances at the both S_1 and S_2 are assumed to be identical; i.e., $\mathcal{P}_{S_1} = \mathcal{P}_{S_2} = \mathcal{P}_S$ and $\sigma_{S_1}^2 = \sigma_{S_2}^2 = \sigma_S^2$.

[21] It is important to note that the random variables $\gamma_{S_1}^{(J,L,m)}$ and $\gamma_{S_2}^{(J,L,m)}$ are not statistically independent.

where $\Psi(x) = \mathrm{e}^{-\left(\frac{qz(p+1)(\alpha\beta z+\eta)}{\zeta_2[\zeta_1 x+(p+1)\phi(z)]}\right)}$. The integral in (47b) can be readily evaluated by using the GLQ rule as $\int_0^\infty \Psi(x)\mathrm{e}^{-x}\mathrm{d}x = \sum_{t=1}^{T_g} w_t \Psi(x_t) + \mathcal{R}_{T_g}$, where $x_t|_{t=1}^{T_g}$ and $w_t|_{t=1}^{T_g}$ are the abscissas and weights of the GLQ, respectively [18, Eq. (25.4.45)]. Specifically, x_t is the tth root of the Laguerre polynomial $\mathcal{L}_n(x)$ [18, Chap. 22], and the corresponding tth weight is given by $w_t = \frac{(\,t!)^2 x_t}{(t+1)^2[\mathcal{L}_{t+1}(x_t)]^2}$. Both x_t and w_t can be efficiently computed by using the classical algorithm proposed in [19]. Further, T_g is the number of terms used in the GLQ summation, and $\mathcal{R}_{T_g}$ is the remainder term, which readily diminishes as T_g approaches as small as 10 [19].

B. By using the Taylor series expansion

The integral in (47a) can be written by applying the Taylor series to $\mathrm{e}^{-\frac{pz(\alpha\beta z+\eta)}{\zeta_2 t}}$ as follows:

$$\mathcal{J}(z) = \sum_{i=0}^{\infty} \frac{(-1)^i}{i!}[acz(\alpha\beta z+\eta)]^i \mathrm{e}^{a\phi(z)} \int_{a\phi(z)}^{\infty} \frac{\mathrm{e}^{-t}}{t^i}\mathrm{d}t, \quad (48a)$$

where α, β and $\phi(z)$ are defined in (9), and $a = \frac{p+1}{\zeta_1}$, $c = \frac{q}{\zeta_2}$. The integral in (48a) can be evaluated by using [21, Eq. (3.381.6)] as

$$\mathcal{J}(z) = \sum_{i=0}^{\infty} \frac{(-1)^i [acz(\alpha\beta z+\eta)]^i \mathrm{e}^{\frac{a\phi(z)}{2}} \mathcal{W}_{\frac{-i}{2},\frac{1-i}{2}}(a\phi(z))}{(i)![a\phi(z)]^{\frac{i}{2}}}, \quad (48b)$$

where $\mathcal{W}_{\nu,\mu}(z)$ is the Whittaker function [21, Eq. (9.220.4)]. Eq. (48b) can be further simplified by using [28] as

$$\mathcal{J}(z) = \sum_{i=0}^{\infty} \frac{(-1)^i}{i!}[acz(\alpha\beta z+\eta)]^i \mathrm{e}^{a\phi(z)} \Gamma(1-i, a\phi(z)), \quad (48c)$$

where $\Gamma(\mu, z)$ is the complementary incomplete gamma function [18, Eq. (8.350.2)].

Next, we test the convergence of the infinite series expansion in (48c) as follows: To this end, we denote the summand of (48c) by $\mathcal{A}_i(z)$.

$$\lim_{i\to\infty} \frac{\mathcal{A}_{i+1}}{\mathcal{A}_i} = \lim_{i\to\infty} \frac{-[acz(\alpha\beta z+\eta)]}{i+1} \frac{\Gamma(-i, a\phi(z))}{\Gamma(-i+1, a\phi(z))} \to 0. \quad (49)$$

Equation (49) follows from the fact that $\Gamma(-i, z)$ is monotonically decreasing with $i \geq 0$ and for a given z, and thus the ratio $\frac{\Gamma(-i,a\phi(z))}{\Gamma(-i+1,a\phi(z))}$ is bounded as $i \to \infty$. Since $\lim_{i\to\infty} \frac{\mathcal{A}_{i+1}}{\mathcal{A}_i} < 1$, by using the Ratio test, it can be shown that the infinite series in (48c) is convergent.

Now, by following similar steps to those of P_1, the second part of (40b) (i.e., P_2) can be evaluated readily. Then the CDF of Z_m can be derived as $F_{Z_m}(z) = P_1 + P_2$.

By identifying that the $Z_m|_{m=1}^{N_R}$ are statistically independent and identically distributed random variables, the CDF of Z in (37) can be derived readily as $F_Z(z) = (F_{Z_m}(z))^{N_R}$ (8).

APPENDIX B
PROOF OF THE CDF OF THE EFFECTIVE E2E SNR OF SS-2

The instantaneous sum-rate of MIMO AF TWRNs in (5) can be approximated at high SNRs as follows [14], [15]:

$$\mathcal{R}^{(j,l,m)} = \frac{1}{2}\sum_{i=1}^{2} \log\left(\gamma_{S_i}^{(j,l,m)}\right) \approx \frac{1}{2}\log\left(\gamma_{S_1}^{(j,l,m)}\gamma_{S_2}^{(j,l,m)}\right). \quad (50)$$

The CDF of approximated effective SNR for the SS-2 can be derived as

$$F_{W'}(w) = \Pr\left[W' = \max_{\substack{1\leq j\leq N_1, 1\leq l\leq N_2 \\ 1\leq m\leq N_R}} \left\{\gamma_{S_1}^{(j,l,m)}\gamma_{S_2}^{(j,l,m)}\right\} \leq w\right]$$
$$= \Pr\left[\max_{1\leq m\leq N_R} \left\{\gamma_{S_1}^{(J,L,m)}\gamma_{S_2}^{(J,L,m)}\right\} \leq z\right], \quad (51)$$

where $\gamma_{S_1}^{(J,L,m)}$ and $\gamma_{S_2}^{(J,L,m)}$ are defined in (38). Next we define and expand W'_m as follows:

$$W'_m = \gamma_{S_1}^{(J,L,m)}\gamma_{S_2}^{(J,L,m)} = \frac{\beta^{-2}X_m^2 Y_m^2}{(\mu X_m + Y_m + \frac{1}{\bar{\gamma}_S})(X_m + \mu Y_m + \frac{1}{\bar{\gamma}_S})}, \quad (52)$$

where X_m and Y_m are defined in (38), and $\mu = \frac{\bar{\gamma}_S + \bar{\gamma}_R}{\bar{\gamma}_S}$ and $\beta = \frac{1}{\bar{\gamma}_R}$. Further, W'_m can be upper bounded as

$$W'_m \leq \frac{\beta^{-2}X_m^2 Y_m^2}{(\mu X_m + Y_m)(X_m + \mu Y_m)}$$
$$= \left(\frac{X_m Y_m}{X_m + Y_m}\right)^2 \left(\frac{(X_m + Y_m)^2}{\beta^2(\mu X_m + Y_m)(X_m + \mu Y_m)}\right)$$
$$\leq \frac{1}{\mu\beta^2}\left(\min(X_m, Y_m)\right)^2 = W_m^{ub}. \quad (53)$$

The last step in (53) follows from the well-known inequality between the harmonic mean and the minimum of two positive variables; i.e., $\frac{X_m Y_m}{X_m + Y_m} \leq \min(X_m, Y_m)$ and $\frac{(X_m+Y_m)^2}{(\mu X_m + Y_m)(X_m + \mu Y_m)} \leq \frac{1}{\mu}$, which follows from $(\mu X_m + Y_m)(X_m + \mu Y_m) = \mu(X_m^2 + Y_m^2) + (1+\mu^2)X_m Y_m \geq \mu(X_m^2 + Y_m^2) + 2\mu X_m Y_m = \mu(X_m + Y_m)^2$, for $\mu \geq 1$ [15].

The CDF of W_m^{ub} in (53) can be derived as follows:

$$F_{W_m}(w) \geq F_{W_m^{ub}}(w) = \Pr\left(W_m^{ub} = \frac{\left(\min(X_m, Y_m)\right)^2}{\mu\beta^2} \leq w\right)$$
$$= \left[1 - \left(1 - F_{X_m}(\beta\sqrt{\mu w})\right)\left(1 - F_{Y_m}(\beta\sqrt{\mu w})\right)\right], \quad (54)$$

where $F_{X_m}(x)$ and $F_{Y_m}(x)$ are the CDFs of X_m and Y_m, which are defined in (45). Next, the CDF of $W^{ub} = \max_{1\leq m\leq N_R}\left\{W_m^{ub}\right\}$ can be derived as follows:

$$F_{W^{ub}}(w) = \left[1 - \left(1 - F_{X_m}(\beta\sqrt{\mu w})\right)\left(1 - F_{Y_m}(\beta\sqrt{\mu w})\right)\right]^{N_R}$$
$$= \left[1 - \left(1 - \left[1 - \mathrm{e}^{-\frac{\beta\sqrt{\mu w}}{\zeta_1}}\right]^{N_1}\right)\left(1 - \left[1 - \mathrm{e}^{-\frac{\beta\sqrt{\mu w}}{\zeta_2}}\right]^{N_2}\right)\right]^{N_R}. \quad (55)$$

By using binomial expansion, $F_{W^{ub}}(w)$ can be derived in closed-form as given in (11).

APPENDIX C
PROOF OF THE HIGH SNR APPROXIMATION OF THE OUTAGE PROBABILITY FOR SS-1

The single polynomial approximation of the CDFs of X_m and Y_m in (45) at the origin can be derived as [33]

$$F_{X_m}^{\infty}(x) = \frac{x^{N_1}}{\zeta_1^{N_1}} + o\left(x^{N_1+1}\right) \text{ and } F_{Y_m}^{\infty}(y) = \frac{y^{N_2}}{\zeta_2^{N_2}} + o\left(y^{N_2+1}\right). \quad (56)$$

Similarly, single polynomial approximations of the PDFs of X_m and Y_m at the origin are given by [33]

$$f_{X_m}^{\infty}(x) = \frac{N_1 x^{N_1-1}}{\zeta_1^{N_1}} + o\left(x^{N_1}\right) \text{ and } f_{Y_m}^{\infty}(y) = \frac{N_2 y^{N_2-1}}{\zeta_2^{N_2}} + o\left(y^{N_2}\right). \quad (57)$$

First, we consider $P_1(z)$ in (41). By substituting (57) and (56) into (41), the single polynomial approximations of $\mathcal{I}_1(z)$ and $\mathcal{I}_2(z)$ at the origin can be derived readily as follows:

$$\mathcal{I}_1^{\infty}(z) = \frac{N_1(\beta z)^{N_1+N_2}}{(N_1+N_2)\zeta_1^{N_1}\zeta_2^{N_2}} + o\left(z^{N_1+N_2+1}\right) \quad \text{and}$$
$$\mathcal{I}_2^{\infty}(z) = \frac{N_1(\alpha z)^{N_1+N_2}}{(N_1+N_2)\zeta_1^{N_1}\zeta_2^{N_2}} + o\left(z^{N_1+N_2+1}\right). \tag{58}$$

Next, the single polynomial approximations of $\mathcal{I}_3(z)$ at the origin can be derived follows: The Integral $\mathcal{I}_3(z)$ in (41) can be re-written by applying a change of variable; $t+\beta z \to t$ as

$$\mathcal{I}_3(z) = \int_{t=\phi(z)+\beta z}^{\infty} \Pr\left[Y_m \le \frac{z(\alpha t+\eta)}{t-\beta z}\right] f_{X_m}(t)\,\mathrm{d}t. \tag{59}$$

Let us consider the single polynomial approximation of $\mathcal{I}_3(z)$ at the origin. If $\lim_{z\to 0^+}$, then $\lim_{\frac{z(\alpha t+\eta)}{t-\beta z}\to 0^+}$. Thus, $\mathcal{I}_3(z)$ in (59) can be approximated at $\lim_{z\to 0^+}$ as follows:

$$\begin{aligned}\mathcal{I}_3^{\infty}(z) &= F_{Y_m}^{\infty}(\alpha z)\left(\lim_{z\to 0^+}\int_{t=\phi(z)+\beta z}^{\infty} f_{X_m}(t)\,\mathrm{d}t\right)\\ &= F_{Y_m}^{\infty}(\alpha z)\left[1-F_{X_m}^{\infty}(\phi(z)+\beta z)\right].\end{aligned} \tag{60}$$

By substituting (56) into (60) and by selecting the lowest powers of z, the single polynomial approximation of $\mathcal{I}_3(z)$ at the origin can be derived as

$$\mathcal{I}_3^{\infty}(z) = \frac{(\alpha z)^{N_2}}{\zeta_2^{N_2}} + o\left(z^{N_2+1}\right). \tag{61}$$

Now, the single polynomial approximation of $P_1(z)$ at the origin is given by $P_1^{\infty}(z) = \mathcal{I}_1^{\infty}(z) + \mathcal{I}_2^{\infty}(z) + \mathcal{I}_3^{\infty}(z)$. In particular, the behavior of $P_1(z)$ at the origin is completely governed by $\mathcal{I}_3^{\infty}(z)$ as it has the lowest powers of z, and thus $P_1^{\infty}(z)$ can be simplified as

$$P_1^{\infty}(z) = \frac{(\alpha z)^{N_2}}{\zeta_2^{N_2}} + o\left(z^{N_2+1}\right). \tag{62}$$

By following similar steps to those of $P_1^{\infty}(z)$, the single polynomial approximation of $P_2(z)$ in (40a) at the origin can be derived as

$$P_2^{\infty}(z) = \frac{(\alpha z)^{N_1}}{\zeta_1^{N_1}} + o\left(z^{N_1+1}\right). \tag{63}$$

Next, the single polynomial approximation of Z_m at the origin can be derived by using (62) and (63) as follows:

$$\begin{aligned}F_{Z_m}^{\infty}(z) &= P_1^{\infty}(z) + P_2^{\infty}(z)\\ &= \begin{cases}\frac{1}{(\zeta_1)^{N_1}}\left(\frac{\bar\gamma_S+\bar\gamma_R}{\bar\gamma_S\bar\gamma_R}\right)^{N_1} z^{N_1} + o\left(z^{N_1+1}\right), & N_1 < N_2\\ \frac{1}{(\zeta_2)^{N_2}}\left(\frac{\bar\gamma_S+\bar\gamma_R}{\bar\gamma_S\bar\gamma_R}\right)^{N_2} z^{N_2} + o\left(z^{N_2+1}\right), & N_1 > N_2\\ \left(\frac{1}{(\zeta_1)^{N}}+\frac{1}{(\zeta_2)^{N}}\right)\left(\frac{\bar\gamma_S+\bar\gamma_R}{\bar\gamma_S\bar\gamma_R}\right)^{N} z^{N} + o\left(z^{N+1}\right), & N_1 = N_2 = N.\end{cases}\end{aligned} \tag{64}$$

Now, the asymptotic outage probability can be derived as in (12a) by first obtaining the single polynomial approximation of Z at the origin by substituting (64) into $F_Z^{\infty}(z) = (F_{Z_m}^{\infty}(z))^{N_R}$ and then evaluating it at γ_{th}.

APPENDIX D
PROOF OF THE HIGH SNR APPROXIMATION OF THE OUTAGE PROBABILITY FOR SS-2

The SNR upper bound in (53) is asymptotically exact (see Section VIII). Thus, the single polynomial approximation of the CDF for the effective SNR of SS-2 can be derived by substituting the single polynomial approximations of the CDFs of X_m and Y_m at the origin in (56) into (55) as follows:

$$\begin{aligned}F_{W_{ub}}^{\infty}(w) = \Bigg[1 - \Bigg(1 &- \left(\frac{(\bar\gamma_S+\bar\gamma_R)w}{\zeta_1^2\bar\gamma_S\bar\gamma_R^2}\right)^{\frac{N_1}{2}} - \left(\frac{(\bar\gamma_S+\bar\gamma_R)w}{\zeta_2^2\bar\gamma_S\bar\gamma_R^2}\right)^{\frac{N_2}{2}}\\ &+ \left(\frac{(\bar\gamma_S+\bar\gamma_R)w}{\zeta_2^2\bar\gamma_S\bar\gamma_R^2}\right)^{\frac{N_1+N_2}{2}} + o\left(w^{\frac{N_1+N_2}{2}+1}\right)\Bigg)\Bigg]^{N_R}.\end{aligned} \tag{65}$$

By expanding (65) and selecting the lowest powers of w, the single polynomial approximation of the CDF for the effective SNR of SS-2 can be derived. By evaluating this asymptotic CDF at γ_{th}, the asymptotic outage probability at high SNRs can be obtained as given in (13a).

APPENDIX E
PROOF OF THE OUTAGE PROBABILITY OF SS-1 WITH FEEDBACK DELAYS

When antennas are selected using outdated CSI due to feedback delays, $\gamma_{S_1}^{(J,L)}$ and $\gamma_{S_2}^{(J,L)}$ in (38) can be expressed as[22]

$$\gamma_{S_1}^{(\hat J,\hat L)} = \max_{1\le j\le N_1, 1\le l\le N_2}\left(\gamma_{S_1}^{(j,l)}\right) = \frac{\hat X\hat Y}{\alpha\hat X+\beta\hat Y+\eta} \quad \text{and}$$
$$\gamma_{S_2}^{(\hat J,\hat L)} = \max_{1\le j\le N_1, 1\le l\le N_2}\left(\gamma_{S_2}^{(j,l)}\right) = \frac{\hat X\hat Y}{\beta\hat X+\alpha\hat Y+\eta}, \tag{66}$$

where $\hat X = \max_{1\le j\le N_1}\left(|\hat h_{S_1R}^{(j)}|^2\right)$, and $\hat Y = \max_{1\le l\le N_2}\left(|\hat h_{S_2R}^{(l)}|^2\right)$. Here, $\hat h_{S_1R}^{(j)}$ and $\hat h_{S_2R}^{(l)}$ are the jth and lth elements of the outdated channel vectors defined in (22). In fact, $\hat X$ and $\hat Y$ are the induced order statistics of original random variables X and Y [27]. Thus, the CDF and the PDF of $\hat X$ can be derived by using techniques similar those used in [29] as follows:

$$F_{\hat X}(x) = 1 - \sum_{p=0}^{N_1-1}(-1)^p\binom{N_1}{p+1}\mathrm{e}^{-\frac{(p+1)x}{\zeta_1(1+p(1-\rho_1^2))}} \quad \text{and}$$
$$f_{\hat X}(x) = \sum_{p=0}^{N_1-1}\frac{(-1)^p N_1\binom{N_1-1}{p}}{\zeta_1\left(1+p\left(1-\rho_1^2\right)\right)}\mathrm{e}^{-\frac{(p+1)x}{\zeta_1(1+p(1-\rho_1^2))}}. \tag{67}$$

Similarly, the CDF and PDF of $\hat Y$ can be derived as

$$F_{\hat Y}(y) = 1 - \sum_{q=0}^{N_2-1}(-1)^q\binom{N_2}{q+1}\mathrm{e}^{-\frac{(q+1)y}{\zeta_2(1+q(1-\rho_2^2))}} \quad \text{and}$$
$$f_{\hat Y}(y) = \sum_{q=0}^{N_2-1}\frac{(-1)^q N_2\binom{N_2-1}{q}}{\zeta_2\left(1+p\left(1-\rho_1^2\right)\right)}\mathrm{e}^{-\frac{(q+1)y}{\zeta_2(1+q(1-\rho_2^2))}}. \tag{68}$$

By substituting (67) and (68) into (41) and following techniques similar to those in Appendix A, the CDF of $\hat Z$, and thereby, outage probability can be derived as given in (23).

[22]Since the system model is relaxed by considering a single-antenna relay, the dependency of e2e SNRs on relay antenna index (m) is ignored.

The single polynomial approximation of $F_{\hat{X}}(x)$ and $f_{\hat{X}}(x)$ at the origin can be derived as

$$F_{\hat{X}}^{\infty}(x)=\sum_{p=0}^{N_1-1}\frac{(-1)^p N_1\binom{N_1-1}{p}}{\zeta_1(1+p(1-\rho_1^2))}x+o\left(x^2\right) \quad \text{and}$$
$$f_{\hat{X}}^{\infty}(x)=\sum_{p=0}^{N_1-1}\frac{(-1)^p N_1\binom{N_1-1}{p}}{\zeta_1(1+p(1-\rho_1^2))}+o\left(x\right). \tag{69}$$

Similarly, the single polynomial approximation of $F_{\hat{Y}}(y)$ and $f_{\hat{Y}}(y)$ at the origin is given by

$$F_{\hat{Y}}^{\infty}(y)=\sum_{q=0}^{N_2-1}\frac{(-1)^q N_2\binom{N_2-1}{q}}{\zeta_2(1+q(1-\rho_2^2))}y+o\left(y^2\right) \quad \text{and}$$
$$f_{\hat{Y}}^{\infty}(y)=\sum_{q=0}^{N_2-1}\frac{(-1)^q N_2\binom{N_2-1}{q}}{\zeta_2(1+q(1-\rho_2^2))}+o\left(y\right). \tag{70}$$

By substituting (69) and (70) into (58) and (60), and following steps similar to those in Appendix C, high SNR approximation of the outage probability can be derived as given in (25a).

Appendix F
Proof of the asymptotic outage probability in correlated fading

In this subsection, the proof of the asymptotic outage probability in correlated fading is sketched. To this end, the CDFs of X_m and Y_m defined in (38) for correlated fading are given by [30], [31][23]

$$F_{X_m}(x)=\int_0^{\infty}\prod_{n=1}^{N_1}\left[1-\mathcal{Q}_1\left(\sqrt{\frac{2\rho_{1,n}t}{1-\rho_{1,n}}},\sqrt{\frac{2x}{\zeta_1(1-\rho_{1,n})}}\right)\right]\mathrm{e}^{-t}\mathrm{d}t, \tag{71a}$$

$$F_{Y_m}(y)=\int_0^{\infty}\prod_{n=1}^{N_2}\left[1-\mathcal{Q}_1\left(\sqrt{\frac{2\rho_{2,n}t}{1-\rho_{2,n}}},\sqrt{\frac{2y}{\zeta_1(1-\rho_{2,n})}}\right)\right]\mathrm{e}^{-t}\mathrm{d}t, \tag{71b}$$

where $\mathcal{Q}_m(a,b)$ is the mth order Marcum-Q function [32, Eq. (1)]. Next, we proceed to derive the single polynomial approximations of $F_{X_m}(x)$ and $F_{Y_m}(y)$ by first developing a single polynomial approximation for $Q_1(\alpha,\beta)$ in (71a) and (71b) as follows: An alternate integral expression for $\mathcal{Q}_1(\alpha,\beta)$ is written as [32, Eq. (A-1)]

$$\mathcal{Q}_1(\alpha,\beta)=1-\int_0^{\beta}x\,\mathrm{e}^{-\frac{x^2+\alpha^2}{2}}\,\mathcal{I}_0(\alpha x)\mathrm{d}x. \tag{72a}$$

Eq. (72a) can now be expanded by using [21, Eq. (8.445)] as

$$\mathcal{Q}_1(\alpha,\beta)=1-\sum_{k=0}^{\infty}\frac{\alpha^{2k}\mathrm{e}^{-\frac{\alpha^2}{2}}}{k!\Gamma(k+1)}\gamma\left(k+1,\frac{\beta^2}{2}\right). \tag{72b}$$

By substituting [21, Eq. (8.354)] into (72b), its infinite series presentation can be derived as

$$\mathcal{Q}_1(\alpha,\beta)=1-\sum_{k=0}^{\infty}\sum_{l=0}^{\infty}\frac{(-1)^l\alpha^{2k}\mathrm{e}^{-\frac{\alpha^2}{2}}\beta^{2(k+l+1)}}{2^{k+1+1}\,l!\,k!\Gamma(k+1)\Gamma(k+l+1)}. \tag{72c}$$

[23]To the best of our knowledge, there appears no closed-form solution for CDF of maximum of $N>3$ correlated exponential random variables. In fact, (71a) and (71b) are the most efficient solutions to this problem [30], [31].

The first order expansion of $\mathcal{Q}_1(\alpha,\beta)$ can be derived by collecting the lowest power of β as [33]

$$\lim_{\beta\to 0}\mathcal{Q}_1(\alpha,\beta)=1-\frac{\beta}{2}\mathrm{e}^{-\frac{\alpha^2}{2}}+o(\beta^3). \tag{72d}$$

Now, by substituting (72d) into (71a) and (71b), the single polynomial expansions of $F_{X_m}(x)$ and $F_{Y_m}(y)$ at the origin can be derived as follows:

$$F_{X_m}^{\infty}(x)=\omega_1\left(\frac{x}{\zeta_1}\right)^{N_1}+o(x^{N_1+1}), \text{ and}$$
$$F_{Y_m}^{\infty}(y)=\omega_2\left(\frac{y}{\zeta_2}\right)^{N_2}+o(y^{N_2+1}), \tag{73}$$

where ω_1 and ω_2 are defined in (30d). Similarly, the corresponding single polynomial expansions of $f_{X_m}(x)$ and $f_{Y_m}(y)$ at the origin are given by

$$f_{X_m}^{\infty}(x)=\frac{N_1\omega_1 x^{N_1-1}}{\zeta_1^{N_1}}+o(x^{N_1}), \text{ and}$$
$$f_{Y_m}^{\infty}(y)=\frac{N_2\omega_2 y^{N_2-1}}{\zeta_2^{N_2}}+o(y^{N_2}). \tag{74}$$

The desired result (30a) can be derived by first substituting (73) and (74) into (41) and then following steps similar to those in Appendix C.

Appendix G
Proof of the overall outage probability over n.i.i.d. fading

In this subsection, the proof of the overall outage probability of joint relay and Tx/Rx antenna selection based on SS-1 for MIMO TWRNs over n.i.i.d. Rayleigh fading is sketched. In this context, the CDF of X_m defined in (38) is expressed as

$$F_{X_m}(x)=\prod_{p=1}^{N_1}\left(1-\mathrm{e}^{-\frac{x}{\zeta_{1,p,m,k}}}\right)$$
$$=1+\sum_{p=1}^{N_1}(-1)^p\sum_{\lambda_1=1}^{N_1-p+1}\sum_{\lambda_2=\lambda_1+1}^{N_1-p+2}\cdots\sum_{\lambda_p=\lambda_{p-1}+1}^{N_1}\mathrm{e}^{-x\sum_{n=1}^{p}\zeta_{1,\lambda_n,m,k}^{-1}}. \tag{75}$$

By employing an efficient short-hand notation [25], (75) can be re-written as

$$F_{X_m}(x)=\sum_{\tau_1\in\mathcal{T}_{p,k}^{N_1}}\mathrm{sign}(\tau_1)\,\mathrm{e}^{-\tau_1 x}. \tag{76a}$$

Similarly, the CDF of Y_m defined in (38) can be written as

$$F_{Y_m}(y)=\sum_{\tau_2\in\mathcal{T}_{q,k}^{N_2}}\mathrm{sign}(\tau_2)\mathrm{e}^{-\tau_2 y}. \tag{76b}$$

In (76a) and (76b), $\mathcal{T}_{a,b}^{c}$ is defined in (35). Moreover, $\mathrm{sign}(\sigma_i)$ and $\mathrm{sign}(\tau_i)$ are the signs of each term in the corresponding expansion of the product terms in (75). Furthermore, the PDFs of X_m and Y_m are given by [25]

$$f_{X_m}(x)=\sum_{p=1}^{N_1}\frac{\mathrm{e}^{-\frac{x}{\zeta_{1,p,m,k}}}}{\zeta_{1,p,m,k}}\sum_{\sigma_1\in\mathcal{S}_{p,u,k}^{N_1}}\mathrm{sign}(\sigma_1)\mathrm{e}^{-\sigma_1 x} \text{ and}$$
$$f_{Y_m}(y)=\sum_{q=1}^{N_2}\frac{\mathrm{e}^{-\frac{y}{\zeta_{2,q,m,k}}}}{\zeta_{2,q,m,k}}\sum_{\sigma_2\in\mathcal{S}_{q,u,k}^{N_2}}\mathrm{sign}(\sigma_2)\mathrm{e}^{-\sigma_2 x}, \tag{77}$$

where the set $\mathcal{S}_{a,b,k}^{N_i}$ is defined in (34).

The desired result (32) can now be derived by substituting (76a), (76b) and (77) into (41) and then by following techniques similar to those in Appendix A.

REFERENCES

[1] B. Rankov and A. Wittneben, "Spectral efficient protocols for half-duplex fading relay channels," *IEEE J. Sel. Areas Commun.*, vol. 25, no. 2, pp. 379–389, 2007.

[2] P. Popovski and H. Yomo, "Wireless network coding by amplify-and-forward for bi-directional traffic flows," *IEEE Commun. Lett.*, vol. 11, no. 1, pp. 16–18, 2007.

[3] S. Berger *et al.*, "Recent advances in amplify-and-forward two-hop relaying," *IEEE Commun. Mag.*, vol. 47, no. 7, pp. 50–56, Jul. 2009.

[4] R. H. Y. Louie, Y. Li, and B. Vucetic, "Practical physical layer network coding for two-way relay channels: performance analysis and comparison," *IEEE Trans. Wireless Commun.*, vol. 9, pp. 764–777, 2010.

[5] M. Ju and I.-M. Kim, "Relay selection with ANC and TDBC protocols in bidirectional relay networks," *IEEE Trans. Commun.*, vol. 58, no. 12, pp. 3500–3511, 2010.

[6] R. Zhang *et al.*, "Optimal beamforming for two-way multi-antenna relay channel with analogue network coding," *IEEE J. Sel. Areas Commun.*, vol. 27, no. 5, pp. 699–712, 2009.

[7] C. Li, L. Yang, and W.-P. Zhu, "Two-way MIMO relay precoder design with channel state information," *IEEE Trans. Commun.*, vol. 58, no. 12, pp. 3358–3363, 2010.

[8] J. Joung and A. Sayed, "Multiuser two-way amplify-and-forward relay processing and power control methods for beamforming systems," *IEEE Trans. Signal Process.*, vol. 58, no. 3, pp. 1833–1846, Mar. 2010.

[9] A. Y. Panah and R. W. Heath, "MIMO two-way amplify-and-forward relaying with imperfect receiver CSI," *IEEE Trans. Veh. Technol.*, vol. 59, no. 9, pp. 4377–4387, 2010.

[10] A. F. Molisch and M. Z. Win, "MIMO systems with antenna selection," *IEEE Microwave*, vol. 5, no. 1, pp. 46–56, 2004.

[11] N. Sollenberger, "Diversity and automatic link transfer for a TDMA wireless access link," in *IEEE Global Telecommun. Conf., Houston. 1993*, Dec. 1993, pp. 532–536.

[12] M. Eslamifar *et al.*, "Performance analysis of two-way multiple-antenna relaying with network coding," in *Proc. IEEE 70th Veh. Tech. Conf. Fall*, 2009, pp. 1–5.

[13] ——, "Max-min antenna selection for bi-directional multi-antenna relaying," in *Proc. IEEE 71st Veh. Tech. Conf.*, 2010, pp. 1–5.

[14] Y. Han *et al.*, "Performance bounds for two-way amplify-and-forward relaying," *IEEE Trans. Wireless Commun.*, vol. 8, pp. 432–439, 2009.

[15] K.-S. Hwang, Y.-C. Ko, and M.-S. Alouini, "Performance bounds for two-way amplify-and-forward relaying based on relay path selection," in *Proc. IEEE 69th Veh. Tech. Conf. VTC Spring*, 2009, pp. 1–5.

[16] Y. Li, R. H. Y. Louie, and B. Vucetic, "Relay selection with network coding in two-way relay channels," *IEEE Trans. Veh. Technol.*, vol. 59, no. 9, pp. 4489–4499, 2010.

[17] D. N. C. Tse, P. Viswanath, and L. Zheng, "Diversity-multiplexing tradeoff in multiple-access channels," *IEEE Trans. Inf. Theory*, vol. 50, no. 9, pp. 1859–1874, 2004.

[18] M. Abramowitz and I. Stegun, *Handbook of Mathematical Functions*. Dover Publications, Inc., New York, 1970.

[19] Golub *et al.*, "Calculation of Gauss quadrature rules," Stanford, CA, USA, Tech. Rep., 1967.

[20] S. Zhou and G. Giannakis, "Adaptive modulation for multiantenna transmissions with channel mean feedback," *IEEE Trans. Wireless Commun.*, vol. 3, no. 5, pp. 1626–1636, Sep. 2004.

[21] I. Gradshteyn and I. Ryzhik, *Table of integrals, Series, and Products*, 7th ed. Academic Press, 2007.

[22] J. Makhoul, "Linear prediction: A tutorial review," *IEEE Proc.*, vol. 63, no. 4, pp. 561–580, Apr. 1975.

[23] T. Ekman, "Prediction of mobile radio channels, modeling and design," Ph.D. dissertation, Uppsala Univ., Uppsala, Sweden, Sept. 2002.

[24] Y. Tong, *The multivariate Normal Distribution*, 3rd ed. New York: Spring-Verlag, 1990.

[25] T. Eng, N. Kong, and L. Milstein, "Comparison of diversity combining techniques for Rayleigh-fading channels," *IEEE Trans. Commun.*, vol. 44, no. 9, pp. 1117–1129, sept. 1996.

[26] G. Amarasuriya, C. Tellambura, and M. Ardakani, "Performance analysis of zero-forcing for two-way MIMO AF relay networks," *IEEE Wireless Commun. Lett.*, vol. 1, no. 2, pp. 53–56, Apr. 2012.

[27] H. A. David, *Order Statistics*, 2nd ed. Wiley, New York, 1981.

[28] [Online]. Available: http://functions.wolfram.com/ HypergeometricFunctions/WhittakerW/03/01/03/

[29] G. Amarasuriya, C. Tellambura, and M. Ardakani, "Feedback delay effect on dual-hop MIMO AF relaying with antenna selection," in *IEEE Global Commun. Conf.*, Miami, FL, USA, Dec. 2010, pp. 1–5.

[30] Y. Chen and C. Tellambura, "Distribution functions of selection combiner output in equally correlated Rayleigh, Rician, and Nakagami-m fading channels," *IEEE Trans. Commun.*, vol. 52, no. 11, pp. 1948–1956, Nov. 2004.

[31] X. Zhang and N. Beaulieu, "Performance analysis of generalized selection combining in generalized correlated Nakagami- m fading," *IEEE Trans. Commun.*, vol. 54, no. 11, pp. 2103 –2112, Nov. 2006.

[32] A. H. Nuttall, "Some integrals involving the Q-function," Naval Underwater Systems Center, New London Lab., Tech. Rep., Apr. 1972.

[33] Z. Wang and G. B. Giannakis, "A simple and general parameterization quantifying performance in fading channels," *IEEE Trans. Commun.*, vol. 51, no. 8, pp. 1389–1398, Aug. 2003.

Gayan Amarasuriya (S'09) received the B.Sc. degree in Electronic and Telecommunication Engineering (with first-class honors) from the University of Moratuwa, Moratuwa, Sri Lanka, in 2006. He is currently working towards the Ph.D. degree at the Electrical and Computer Engineering Department, University of Alberta, AB, Canada. His research interests include design and analysis of new transmission strategies for cooperative MIMO relay networks and physical layer network coding.

Chintha Tellambura (SM'02-F'11) received the B.Sc. degree (with first-class honors) from the University of Moratuwa, Moratuwa, Sri Lanka, in 1986, the M.Sc. degree in electronics from the University of London, London, U.K., in 1988, and the Ph.D. degree in electrical engineering from the University of Victoria, Victoria, BC, Canada, in 1993.

He was a Postdoctoral Research Fellow with the University of Victoria (1993-1994) and the University of Bradford (1995-1996). He was with Monash University, Melbourne, Australia, from 1997 to 2002. Presently, he is a Professor with the Department of Electrical and Computer Engineering, University of Alberta. His research interests include Diversity and Fading Countermeasures, Multiple-Input Multiple-Output (MIMO) Systems and Space-Time Coding, and Orthogonal Frequency Division Multiplexing (OFDM).

Prof. Tellambura is an Associate Editor for the IEEE Transactions on Communications and the Area Editor for Wireless Communications Systems and Theory in the IEEE Transactions on Wireless Communications. He was Chair of the Communication Theory Symposium in Globecom'05 held in St. Louis, MO.

Masoud Ardakani (M'04-SM'09) received the B.Sc. degree from Isfahan University of Technology in 1994, the M.Sc. degree from Tehran University in 1997, and the Ph.D. degree from the University of Toronto, Canada, in 2004, all in electrical engineering. He was a Postdoctoral fellow at the University of Toronto from 2004 to 2005. He is currently an Associate Professor of Electrical and Computer Engineering and Alberta Ingenuity New Faculty at the University of Alberta, Canada, where he holds an Informatics Circle of Research Excellence (iCORE) Junior Research Chair in wireless communications. His research interests are in the general area of digital communications, codes defined on graphs and iterative decoding techniques. Dr. Adrakani serves as an Associate Editor for the IEEE Transactions on Wireless Communications and the IEEE Communication Letters.